2011

MECHANICAL CHARACTERIZATIONS OF ENVIRONMENTALLY CONDITIONED SHAPE MEMORY POLYMERS FOR RECONFIGURABLE AEROSPACE STRUCTURES

Jared T. Fulcher
University of Kentucky, jared.fulcher@gmail.com

ABSTRACT OF THESIS

MECHANICAL CHARACTERIZATIONS OF ENVIRONMENTALLY CONDITIONED SHAPE MEMORY POLYMERS FOR RECONFIGURABLE AEROSPACE STRUCTURES

Shape memory polymers (SMPs) have been candidate materials for morphing applications. However, the SMPs have not been fully tested to work in relevant environments required for Air Force missions. In this study, an epoxy-based SMP was separately exposed to moisture, lubricating oil and UV radiation, which are simulated service environments designed to be reflective of anticipated performance requirements. The thermomechanical properties and shape memory effects were studied by using novel high-temperature nanoindentation technique. Results show that environmental conditions have affected the glass transition temperature and mechanical properties of the SMPs. In most cases, the conditioned SMPs exhibited higher elastic moduli than the unconditioned SMP. The shape recovery ability of the SMP was assessed by creating an indent and then observing the corresponding recovery according to the standard shape memory cycle. It was found that the deformation was mostly recovered for both conditioned and unconditioned SMP samples on heating the material above its glass transition temperature.

KEYWORDS: Shape Memory Polymer, Nanoindentation, High-Temperature Nanoindentation, Environmental Conditioning, Shape Recovery Ability

Jared T. Fulcher

January 26, 2011

MECHANICAL CHARACTERIZATIONS OF ENVIRONMENTALLY CONDITIONED SHAPE MEMORY POLYMERS FOR RECONFIGURABLE AEROSPACE STRUCTURES

By

Jared T. Fulcher

Dr. Y Charles Lu
Director of Thesis

Dr. James McDonough
Director of Graduate Studies

January 26, 2011

RULES FOR THE USE OF THESES

Unpublished theses submitted for the Master's degree and deposited in the University of Kentucky Library are as a rule open for inspection, but are to be used only with due regard to the rights of the authors. Bibliographical references may be noted, but quotations or summaries of parts may be published only with the permission of the author, and with the usual scholarly acknowledgments.

Extensive copying or publication of the thesis in whole or in part also requires the consent of the Dean of the Graduate School of the University of Kentucky.

A library that borrows this thesis for use by its patrons is expected to secure the signature of each user.

Name	Date

THESIS

Jared T. Fulcher

The Graduate School

University of Kentucky

2011

MECHANICAL CHARACTERIZATIONS OF ENVIRONMENTALLY CONDITIONED SHAPE MEMORY POLYMERS FOR RECONFIGURABLE AEROSPACE STRUCTURES

THESIS

A thesis submitted in partial fulfilment of the requirements
for the degree of Master of Science in
Mechanical Engineering in the College of Engineering at the
University of Kentucky

By

Jared T. Fulcher

Lexington, Kentucky

Director: Dr. Y. Charles Lu, Assistant Professor of Mechanical Engineering

Lexington, Kentucky

2011

This thesis is dedicated to the memory of my mother, Donna Fulcher, who taught me to always persevere and to always to do more than what is expected of you.

ACKNOWLEDGEMENTS

I would like to express my deepest gratitude and respect to my academic advisor Dr. Y. Charles Lu, who not only provided unwavering support and invaluable advice through my undergraduate and graduate academic career, but also gave me this great opportunity to further my post- baccalaureate education at the University of Kentucky.

I would like to thank the American Society of Engineering Education – Air Force Summer Faculty Fellowship Program (SFFP) and the NASA EPSCoR Research Infrastructure Development (RID) Program and Kentucky Space Grant Consortium (KSGC) for the generous support that made this project possible.

Lastly, I would like to express great appreciation to Dr. John Baker and Dr. Haluk Karaca for accepting to be part of my thesis committee, and for their time in spite of their busy schedules.

TABLE OF CONTENTS

LIST OF TABLES

LIST OF FIGURES

CHAPTER ONE INTRODUCTION

1.1 BACKGROUND

Over the last two decades a major push has been made to develop highly adaptive vehicles for aerospace and space applications. These new reconfigurable vehicles will be able to meet multiple mission goals, where in the past, numerous vehicles would be needed to accomplish the same goals. With the development of these adaptive air vehicles, new materials are needed to help take concept to reality. Shape memory polymers (SMPs) are a class of shape memory materials (SMMs) that can recover their shape from a deformed state back to their permanent shape when exposed to the appropriate stimulus (Figure 1.1). Recently, SMPs have been increasingly studied to be adapted to these reconfigurable air vehicles. SMPs can recover large strains (reported 200%); cost less to produce, and their material properties can be tailored to a variety of applications (Lei et al, 2007). These attributes make SMPs much more desirable than conventional shape memory alloys (SMAs). A spider plot representing the proposed capability of an air vehicle with reconfigurable wings can be seen in Figure 1.2 (Thill et al, 2008).

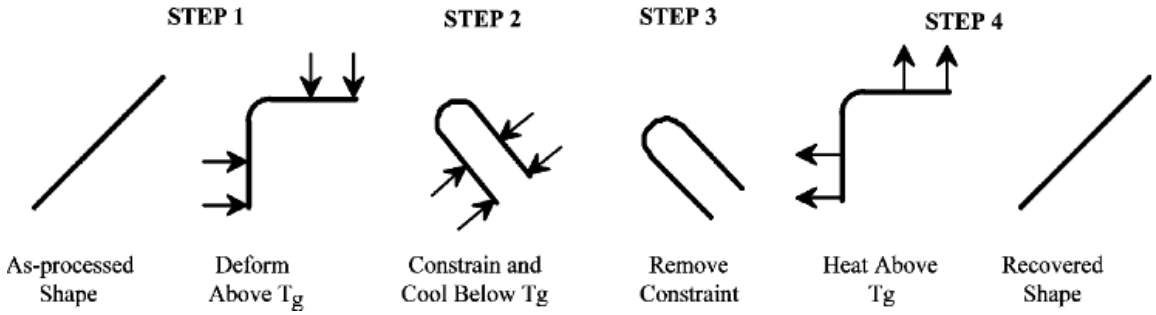

Figure 1.1. Diagrammatic representation of the thermomechanical cycle of a SMP.

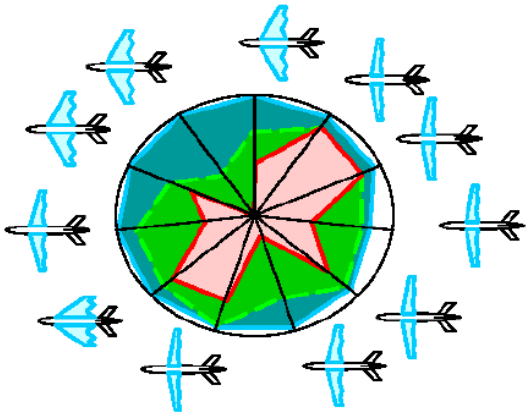

Figure 1.2. Spider plot representing the capabilities of a reconfigurable air vehicle (Thill et al, 2008).

To meet the requirements for the aerospace missions, the SMPs need to be tested in anticipated service environment (water, lubricants, UV light, etc.). Like conventional polymers, the shape memory polymers will undergo physical and chemical aging when exposed to simulated service environments. So far, little work has been done to characterize the material response and affect on material properties after being exposed to the anticipated service conditions for aerospace applications. Air Force testing procedures require the materials to be exposed to certain expected service conditions, i.e., lubricants, water and UV radiation. Correct testing also required that this conditioning be performed at extreme operating temperatures, around 49°C (120°F). Furthermore, although SMPs have been intensively studied over the last twenty years, not until the last few years have small scale experiments been preformed (Atli, et al., 2009; Behl and Lendlein, 2007; Beloshenko, et al., 2005; Gall, et al., 2004; Lendlein and Kelch, 2002; Liu, et al., 2007; Ratna and Karger-Kocsis, 2008; Tobushi, et al., 1996, 1998; Wei, et al., 1998). To help fully develop a working concept of the reconfigurable air vehicle, the localized response of the SMP may prove important.

For examination of the material response of unconditioned and environmentally conditioned SMPs, nanoindentation technique was used. Nanoindentation is a widely accepted technique to evaluate the material properties of SMPs at small-scale. This small-scale test is particularly useful for examining the spatial dependent deformation as

a result of environmental conditioning. For the physical material response or shape recovery examination of the SMP, novel high-temperature nanoindentation was utilized. The shape recovery of SMPs has been studied quite well, but most studies only consider deforming the specimen at ambient temperatures and not at temperatures above the transition temperature. The study of these environmentally conditioned SMPs will prove paramount in the advancement of the work to develop operationally reconfigurable air vehicles.

1.2 OBJECTIVES OF THE THESIS

The recent increase of interest in the development of high adaptive air vehicles has spawned a surge in research involving smart materials. Characterization of these smart materials will directly affect the production and performance of the new generation of reconfigurable air vehicles. Shape memory polymers are one class of materials being considered for the adaptive applications. Under Air Force testing procedures the materials in question need to be tested under anticipated service conditions. These service conditions included exposure to lubricants, water, and UV radiation. Furthermore, the exposure should be conducted at expected service temperatures, which are 49°C (120°F).

To fully characterize the material response of the SMP, two different nanoindentation techniques were used. First, the material properties of the conditioned SMP were examined using standard nanoindentation techniques. The nanoindentation technique has been widely accepted as a standard procedure for characterizing the properties of a material at nano-scale. Further characterization was performed using novel high-temperature nanoindentation technique. The high-temperature nanoindentation was used to evaluate the shape recovery ability of the SMP once conditioned. The results of this study will be used to determine the level of durability of the SMP under expected service conditions.

1.3 ORGANIZATION OF THE THESIS

Chapter 2 of this thesis presents a review of literature concerning the development of SMPs and the application of reconfigurable air vehicles. Chapter 3 provides a synopsis of the conditioning process used for all the SMP specimens. Specimen preparation prior to conditioning is also discussed in Chapter 3. The methods used to characterize the thermomechanical properties of the SMP are presented in Chapter 4. Chapter 5 is dedicated to the shape recovery ability of the environmentally conditioned SMP. Chapter 6 is a review of the results of this study and a brief summary of possible future work.

CHAPTER TWO REVIEW OF LITERATURES

2.1 INTRODUCTION TO SHAPE MEMORY POLYMERS

Shape memory materials (SMMs) are a class of active materials that have dual-shape capability. The dual-shape capability, or shape memory effect, is characterized by the ability to recover a permanent shape from an initial level of pre-deformation when exposed to the appropriate external stimulus. Certain polymers, metal alloys, ceramics, and gels can be classified as SMMs (Lendlein and Kelch, 2002). Of all SMMs, shape memory alloys (SMAs) and shape memory polymers (SMPs) are by and large the most widely studied. The shape memory effect was seen in metal alloys as early as 1951, and the shape memory effect in polymers was reported a decade earlier. However, SMAs are more prominent and more widely used than SMPs (Lei et al., 2007). Shape memory alloys and polymers vary in nearly every material aspect from the basic mechanism for the shape memory effect to the capability of tailoring specific material properties (i.e. elastic modulus and transition temperature). Looking at the basic material characteristics of SMAs and SMPs, it becomes very apparent that the properties of SMPs are more desirable. SMAs have been reported to have high stiffness, high cost, complicated processing demands, and very low recoverable strains, on average less than 8% (Lei et al., 2007). In direct contrast, SMPs are generally low cost, low density, and can recover strain levels of nearly 200% (Lei et al., 2007). Other advantages of SMPs are the ability to specially adapt material properties for specific applications, and SMPs do not require costly or complicated procedures of manufacturing. Furthermore, SMPs can be activated by several stimuli including heat, light, chemical, or perhaps a combination of these stimuli. Additionally, most SMPs are biocompatible and biodegradable (Huang et al., 2010). Accordingly, all of these advantages lead to SMPs being capable of application in a variety of areas.

Thermally induced SMPs are the first polymers reported to show the shape memory effect, and consequently these SMP are the most widely studied and used (Ratna and Karger-Kocsis, 2008). The thermomechanical cycles used to quantify the shape memory

effect of SMPs have been well documented in the literature (Atli, et al., 2009; Behl and Lendlein, 2007; Beloshenko, et al., 2005; Gall, et al., 2004; Lendlein and Kelch, 2002; Liu, et al., 2007; Ratna and Karger-Kocsis, 2008; Tobushi, et al., 1996, 1998; Wei, et al., 1998). Traditionally, there are two types of recovery studied when considering shape recovery: constrained and free. Constrained recovery involves the measurement of the stress produced in the SMP when recovery is activated while the temporary deformation is constrained. This style of recovery would be useful when considering applications where the SMPs are used as actuators. Free recovery involves the recovery of the SMP while under zero constraint. Deployable applications are considered to be examples of free recovery situations. Figure 2.1 presents a graphic representation of the thermomechanical cycle of a SMP subjected to free recovery. The SMP is first activated at a deformation temperature, T_d, which should be above the SMP's glass transition temperature, T_g. Second, the constrained SMP is cooled to a storage temperature, T_s, which is less than T_g. Next the SMP is heated to a recovery temperature, T_r, to allow the free recovery. In general, a range of temperatures may be used for the recovery temperature to allow the SMP to recover its initial permanent shape through heating.

The shape memory effect is not a specific property of any single polymer; instead the shape memory effect results from a combination of polymer structure and polymer morphology together with applied processing and programming (Lendlein and Kelch, 2002). Although, most polymers present a degree of shape memory ability, cross-linking polymers can achieve a higher order of recoverability. Several studies (Behl and Lendlein, 2002; Liu et al., 2007; Lendlien and Kelch, 2002) gave an in-depth discussion of the physical system that results in the shape memory effect in thermally induced SMP. The shape memory effect in thermal induced cross-linked polymers is a result of the transition from a state dominated by entropic energy (rubbery state) to state where internal energy dominates (glassy state) as temperature decreases. Figure 2.2 presents a schematic of the molecular mechanism for a thermally induced cross-linked SMP.

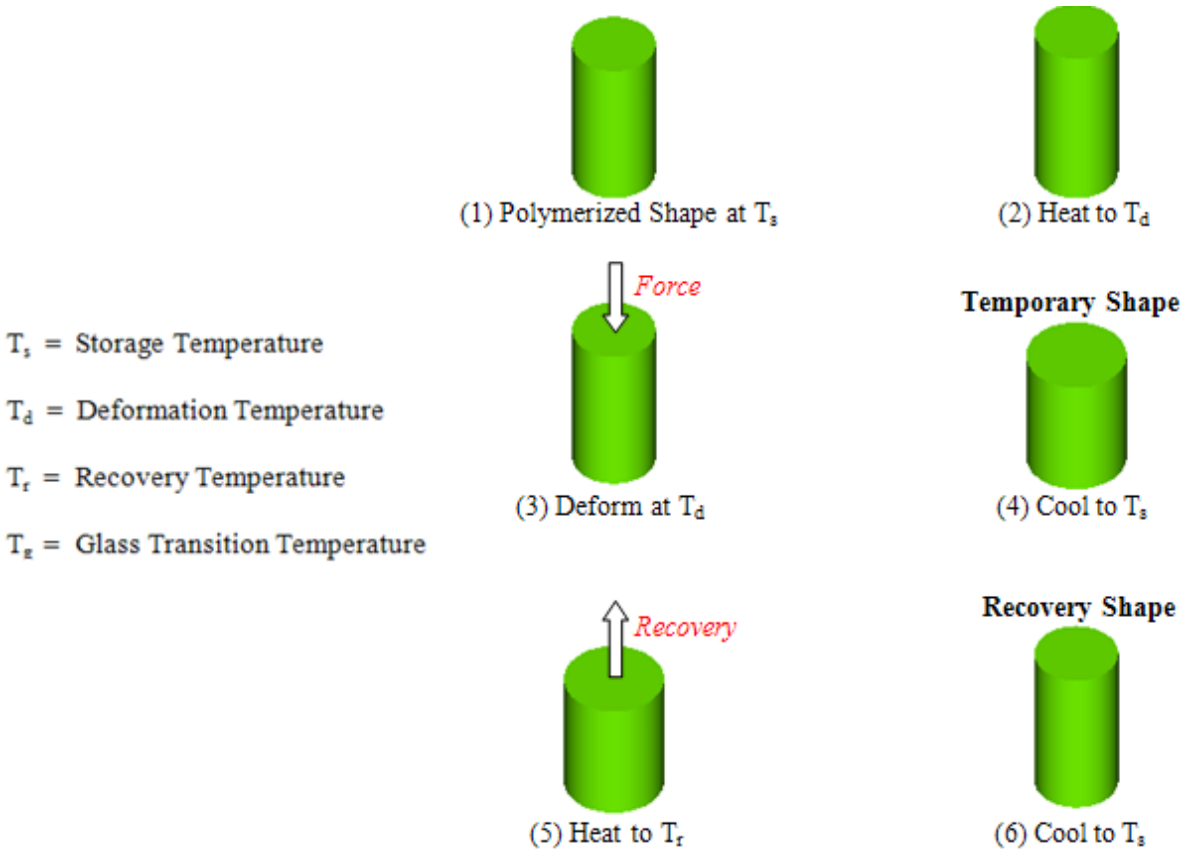

Figure 2.1. Diagram of thermomechanical cycle during free recovery for thermally induced SMP.

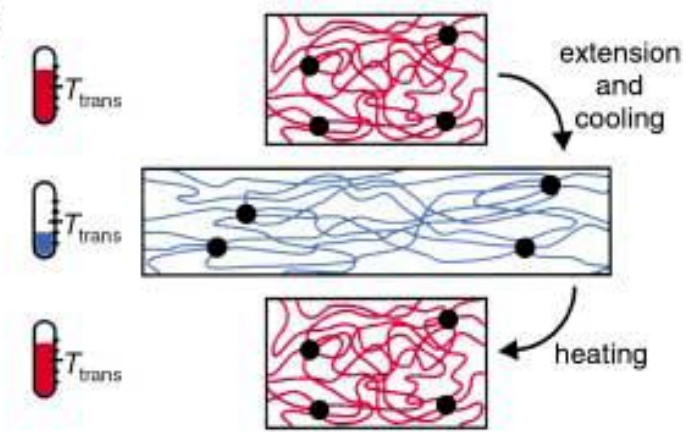

Figure 2.2. Molecular model of shape memory process for thermally induced SMP (Lendlein and Kelch, 2002).

The permanent shape of a SMP is stabilized by cross-linking netpoints denoted by the black points in Figure 2.2. At temperatures above the glass transition temperature, T_g, the molecular chains are flexible and can slip off of each other. An entropy loss occurs as the polymer is deformed under these conditions, which corresponds to entropy elasticity. While in the rubbery state, if the applied load is removed the polymer will tend to recover its permanent shape, and thus recover the entropy lost. However, this recovery process can be interrupted by decreasing the temperature below T_g. Below T_g the molecular chains are frozen, but if the temperature is again increased above T_g the molecular chains will become flexible and return the original configuration based upon the cross-linking net points (Lendlein and Kelch, 2002; Beloshenko et al., 2005).

2.2 AIR VEHICLE RECONFIGURATION (OR MORPHING) WITH SHAPE MEMORY POLYMERS

Shape memory polymers have been considered for a variety of applications because they are easier to manufacture and have a lower cost than other materials, such as shape memory alloys and shape memory ceramics (Huang et al., 2010). Considering the attractive advantages of large deformation and light weight, SMPs are of significant interest in applications in the aerospace field. Within the last 10-15 years the morphology of aircraft wings has become a topic of increased interest. The ability to change wing geometry would allow a single air vehicle to be capable of meeting several performance parameters (Thill et al., 2008). During the mid-1990's, NASA began to fund projects dedicated to the research and development of advanced materials to be adapted to applications in reconfigurable air vehicles. The launch of NASA's "Aircraft Morphing" project (later known as simply "Morphing" project) coincided with the launch of several programs aimed at the development and application of smart materials and structures by the Defense Advanced Research Projects Agency, DARPA. In 2001, NASA released its visualization of a future concept for morphing air vehicle, which can be seen in Figure 2.3 (McGowan et al., 2009).

Figure 2.3. Morphing aircraft concept by NASA (McGowan et al., 2009).

The first comprehensive study of the development of a morphing air vehicle was undertaken in 2001 by DARPA, NASA, and AFRL. The program spanned 8 years and resulted in the development of a full-scale morphing aircraft that utilized SMAs to activate over 70 different wing geometries. The final version of the wing consisted of 10 segments of SMA material arranged in a honeycomb design encased in a silicon skin. Deflection rates of 80 degrees per second were obtained with a maximum deflection of about 20 degrees. It was also concluded that further research was needed to obtain better configurations for the morphing and actuating systems (Kudva, 2004). Figure 2.4 presents several of the resulting wing geometries achieved by activating various segments of the SMA-actuated wing.

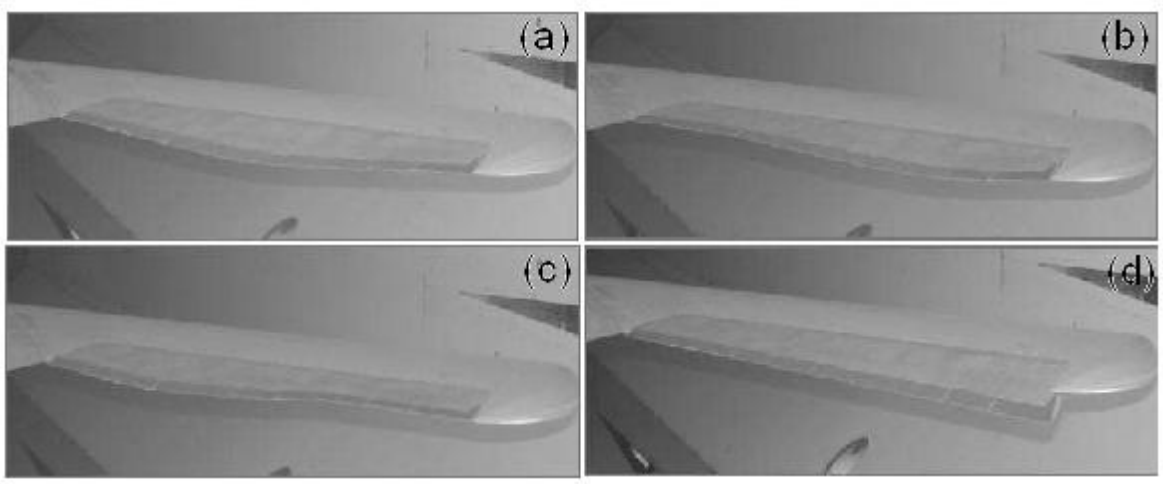

Figure 2.4. (a) 15 degree deformation in the center of wing. (b) 10 degree deformation near the right end of the wing. (c) 10 degree deformation near the left end of the wing. (d) 20 degree deformation at the right end of the wing, (Kudva, 2004).

Another leader in the advancement of morphing structures through the last decade is Cornerstone Research Group (CRG), located in Dayton, OH. CRG has focused the adaption of shape memory materials, primarily SMPs, for many applications including reconfigurable aerospace applications. SMPs seem to be more advantageous for reconfigurable aerospace applications because of their inherently light weight and capability of tailoring their mechanical properties. Recently, CRG has developed a deployable wing using Veritex shape memory composite, which uses CRG's Veriflex SMP has a matrix. Figure 2.5 presents a diagram of the deployable SMP composite wing (CRG, 2010).

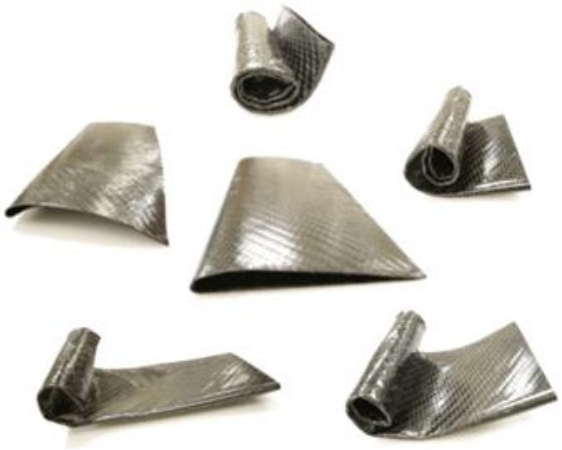

Figure 2.5. CRG's Veritex deployable shape memory composite wing (CRG, 2010).

Conerstone Research Group has also developed a seamless skin for use on a morphing air wing using Veriflex SMP. Utilizing the SMP along with the underlying "sliding rib" structure allows the wing geometry to be changed by seqeuntial heating, deforming, and cooling (CRG, 2010). Figure 2.6 represents a schematic of the "sliding rib" structure with a seamless Veriflex skin.

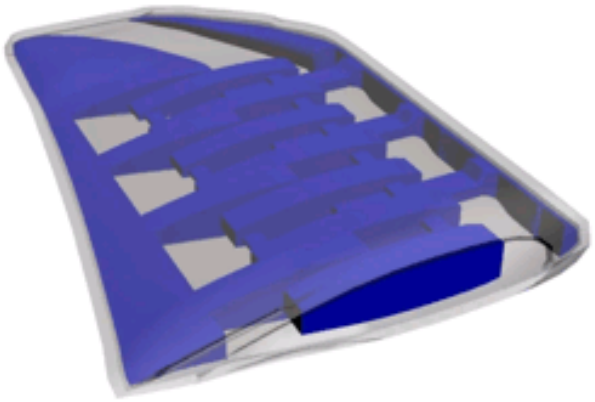

Figure 2.6. Schematic of reconfigurable SMP wing with "sliding rib" sub-sturcture (CRG, 2010).

2.3 THERMOMECHANICAL CHARACTERIZATION OF SHAPE MEMORY POLYMERS

To successfully advance intergration of SMPs into aerospace applications, basic understanding of the thermomechanical responses of SMPs are of the utmost importance. Several quanities are considered when determining the thermomechanical response of a SMP including shape fixity, strain recovery (constrained and/or unconstrained), and shape recovery. The shape fixity is a measure of the ability of the SMP to retain its deformed shape after deforming. Strain recovery corresponds to the SMP's ability to recover a strain once cycled through the appropriate thermomechanical cycle. An extension of the strain recovery is the measure of shape recovery, which is the SMP's ability to recover the deflection experienced during the thermomechanical cycle (Lendlein and Kelch, 2002).

Recently, the shape memory effect of SMPs at small scales has been increasingly studied, mostly through the micro-/nano-indentation technique. Much of the work performed involves looking at the shape recovery of SMPs when deformed below the T_g (Nelson and King, 2005; Wornyo et al., 2007; Yang et al., 2008). The deformed specimens are then heated up above T_g through an additional heating source, and the shape recovery effects are examined. It is noted that such tests are inconsistent with the correct thermomechanical cycle as illustrated in Figure 2.1. Gall et al. (2004) conducted a study were the SMP was indented at both a temperature above and below the glass transition temperature. It was found the indented SMP experience a 100% recovery when indented at 37% of T_g. However, it was noted that the strain level for the ambient deformation needed to be much lower due to increased risk of permanent damage. It may be true that a SMP can be deformed at ambient conditions, but that deformation is limited due to the SMP being in its glassy state. Hence, to be able to achieve the desirable large deflections the SMP should be cycled according to the proposed thermomechanical cycle seen in Figure 2.1. Through novel high temperature nanoindentation, nano-scale indents can be made and subsequently recovered according to the correct thermomechanical cycle.

As a well established method for characterizing the deformation of materials and structure in small scales, nanoindentation is still somewhat limited to measuring the mechanical properties at ambient temperature. Only a limited amount of literature is available addressing the use of high temperature nanoindentation. Schuh et al. (2006) has recently conducted a comprehensive study on high temperature nanoindentation on fused silica. The purpose of that work was mainly to quantify the thermal stability of the indentation equipment. Beake and Smith (2002) have reported the high temperature nanoindentation experiments on fused silica and soda-lime glass. Volinsky et al. (2004) and Sawant and Tin (2008) have recently reported the uses of high temperature nanoindentation on characterizing the mechanical properties of hard thin films and single crystal super-alloys. Recently, the high temperature nanoindenter has been used to measure the mechanical properties of polymer resins at elevated temperatures (Lu et al., 2009).

Although, a substantial amount of work has been done to characterize the thermomechanical properties and response of SMPs, a limited number of studies have been completed on the durability of SMPs under expected service conditions. The response of a SMP's thermomechanical characteristics could vary greatly depending on the environmental conditions. Like conventional polymers, the shape memory polymers will undergo physical and chemical aging when exposed to simulated service environments (Pretch et al., 2009; Tandon et al., 2009; Meents et al., 2009). Pretch et al. have presented results considering the effect of water content in SMPs. It was seen that as the amount of freezable water increased within the SMP samples shape recovery ability decreased. Tandon et al. have proposed the environmental conditions for expected aerospace applications and performed durability assessment of the SMPs by using large scale tensile tests.

To meet the requirements for Air Force missions, the SMPs need to be tested in anticipated service environments (water, lubricants, UV light, etc.). Furthermore, correct environmental conditioning requires exposure to the expected elements at extreme operating temperature, around 49°C (120^{o}F). The present study is to examine the shape-

memory ability and mechanical properties of an epoxy-based SMP before and after separate environmental exposure to (i) water, (ii) lube oil and (iii) UV radiation. Novel high temperature nanoindentation tests will be used. The assessment of these attributes will directly affect the development and utilization of the SMPs for reconfigurable systems.

CHAPTER THREE OVERVIEW OF ENVIRONMENTAL CONDITIONING OF SMPS

3.1 INTRODUCTION

The following chapter presents an overview of the specific shape memory polymer chosen for this study, a description of sample preparation for the nanoindentation testing, and a summary of the conditioning procedure for each specimen. Through examination of the SMP before and after conditioning, the effect of in-service environment on the mechanical properties and shape recovery ability can be evaluated.

3.2 MATERIALS

The SMP chosen for this study was an epoxy-based thermosetting resin (Veriflex-E) developed by the Cornerstone Research Group, Inc. (CRG). Neat resin plaques measuring 30 cm by 30 cm with an average thickness of 3.2 mm were produced using the manufacturer's suggested cure cycle. All testing samples were acquired from these neat resin plaques.

3.2.1 NANOINDENTATION SAMPLE PREPARATION

From the large resin plaque, smaller SMP specimens measuring 1 cm x 1 cm x 3.2 mm were cut using a diamond saw with distilled water as a lubricating and cooling media. Once cut, the smaller plaques' surface was polished in preparation for the nanoindentation test and shape recovery experiments. Surface preparation is of great consequence during nanoindentation because of the scale of the displacement of the indenter. Imperfections in the surface could lead to inconsistent results during experimentation.

The surface polishing was conducted in three stages, with each stage corresponding to a finer quality polishing media. First, each freshly cut plaque was roughly polished using 600 grit sandpaper. This stage was to remove all rough edges left by cutting the plaques

with the diamond saw. The next stage was performed using a table-top polisher with a 0.3 μm deagglomerated alpha alumina polishing media. The table-polisher speed was set at approximately 250 rpm and each specimen was polished for approximately 10 minutes. The final stage of polishing was performed using a Buehler Vibromet 2 vibrating polisher with the same 0.3 μm alumina polishing media.

3.3 ENVIRONMENTAL CONDITIONING

It has been well documented that polymeric materials experience some level of degradation due to in-service conditions. Some of these in-service conditions, such as high temperature, pressure, and moisture, can limit the operational life of these materials. The following procedures have been developed to reflect the expected environmental conditions that a SMP would experience as a component of a reconfigurable aircraft. The smaller SMP samples were conditioned according to the following protocols:

3.3.1 UNCONDITIONED

Some samples of the Veriflex-E SMP were left unconditioned to assess baseline measurements for comparison and to establish correct testing procedures.

3.3.2 WATER CONDITIONING

In order to evaluate the hot-wet performance of SMPs, specimens were immersed in water at 49°C for four days (following the water immersion procedure described in MIL-PRF-23377H paragraph 4.6.6.). Care was taken to ensure that the water used for the immersion met ASTM D 1193 Type IV water with a minimum of 0.2 MOhm electrical resistivity.

3.3.3 UV RADIATION EXPOSURE

The accelerated weathering conditioning was performed in a Xenon-Arc exposure chamber. It was decided to expose only one side of the specimens to UV radiation. The standard exposure cycle is 102 minutes of light only followed by 18 minutes of light and water spray. High purity deionized (DI) water with a minimum of 16.5 MegOhms-cm

resistivity was used. During the light only, the black panel temperature in the exposure chamber was controlled to 63°C ± 2.5°C, and the intensity of the spectral irradiance was controlled to 0.3 to 0.4 watts/meter^2 at a wavelength of 340 nm. Humidity in the chamber was not controlled. Exposure length was limited to 125 cycles.

The nanoindentation specimens were placed on plates, as to allow only one side of the specimens to be UV exposed. Due to the scale of the nanoindentation tests exposure of only one surface of the specimen is acceptable.

3.3.4 Lube Oil Conditioning

SMP specimens were immersed in MIL-L-23699 lubricating oil at 49°C for 24 hours. In addition, some selected specimens were also immersed in lube oil at room temperature to isolate the influence of lubricating oil alone.

3.4 Physical Effects of Environmental Conditioning

Following conditioning, the specimens were wiped dry with a paper towel and evaluated for any visible damage and apparent color changes. Measurements were taken to help quantify any volumetric or weight changes associated with the conditioning process. Table 3.1 presents a summary of the precent change associated with volume and weight for each of environmental conditions. The percentages presented are an average of measurements taken of six samples of each condition. A negative value indicates a loss, while a positive value corresponds to a gain.

Table 3.1. Summarization of volume and weigh change for SMP sample undergoing environmental conditioning.

Condition	UV Exposed for 125 Cycles	Oil Conditioned for 24 Hours @ 25°C	Oil Conditioned for 24 Hours @ 49°C	Water Conditioned for 4 Days @ 49°C
Volume Change (%)	-0.278	0.2541	0.2815	-0.1184
Weight Change (%)	-0.0968	-0.1243	-0.1366	-0.3132

Figure 3.1 shows photographs of the epoxy-based SMP specimens in each conditioned state. The UV exposed specimens are observed to develop a yellow tint throughout the entire volume, which is likely a result of the chemical interaction of UV light with the polymer resin. The apparent color change corresponding to the UV conditioning can be further seen in Figure 3.2. Furthermore, with the use of a Wyko Optical Surface Profiler (Veeco Instruments, Inc.) a noticeable change to the surface of the UV exposed sample can be seen (Figure 3.3). There is no apparent color change or surface degradation in specimens conditioned in water and lube oil.

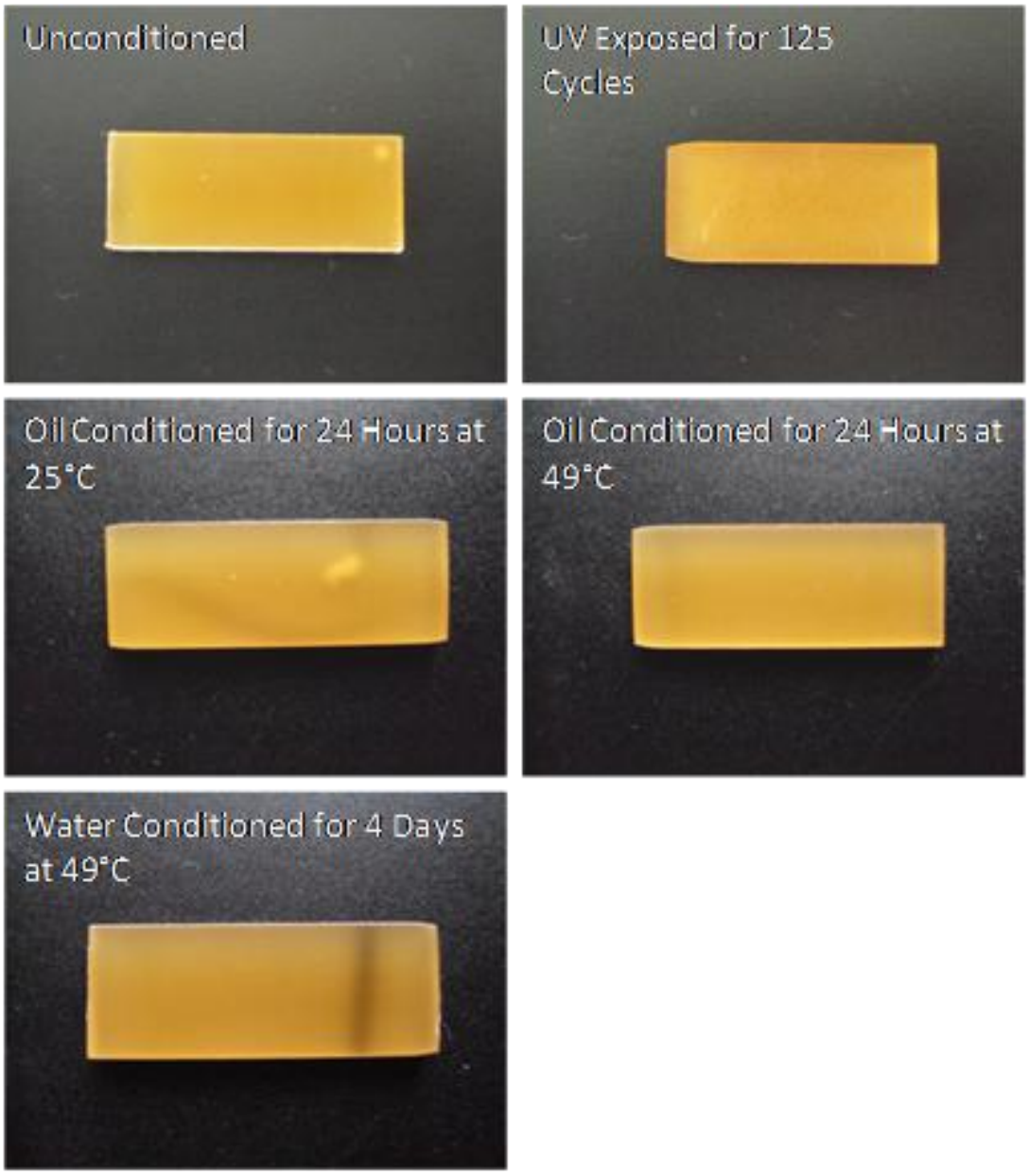

Figure 3.1. Photographs of the unconditioned and conditioned specimens.

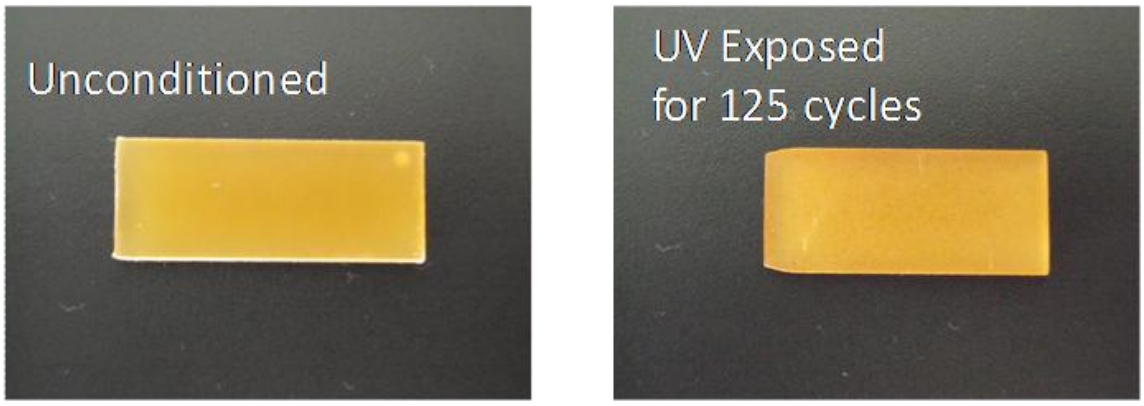

Figure 3.2. The unconditioned and UV conditioned samples are presented here to indicate the appearance of the yellow tint after UV exposure.

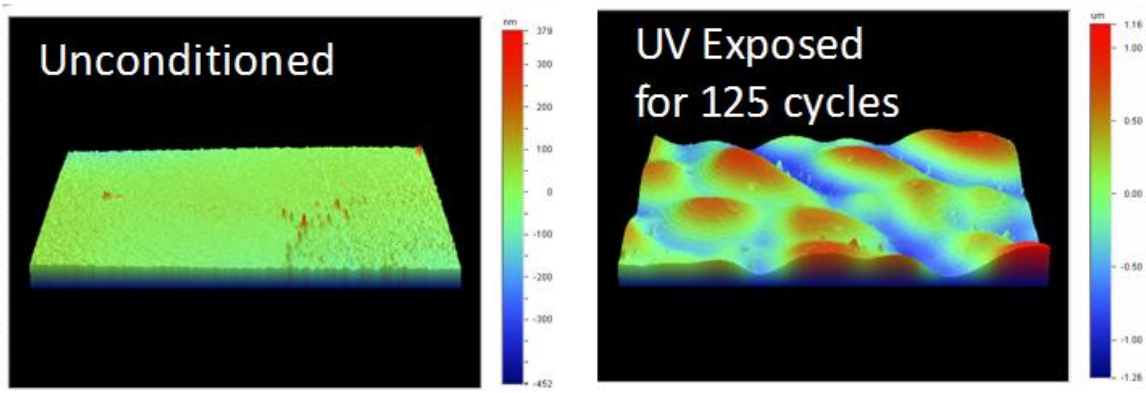

Figure 3.3. The unconditioned and UV conditioned samples are displayed to show the increase in surface roughness after UV exposure.

CHAPTER FOUR THERMOMECHANICAL PROPERTIES OF ENVIRONMENTALLY CONDITIONED SMPS

4.1 INTRODUCTION

This chapter presents the equipment, testing procedures, and results for the thermomechanical response of the Veriflex-E SMP. First, the transition temperature, T_g, and storage modulus for the unconditioned and conditioned SMP samples are established using dynamic mechanical analysis (DMA). Next, the elastic modulus of the unconditioned and conditioned SMP samples is further studied through nanoindentation. A brief review of the appropriate nanoindentation techniques to be applied when testing viscoelastic materials is discussed. The results of the DMA testing and nanoindentation tests are compared to discern any significant changes of the thermomechanical responses for the conditioned Veriflex-E samples.

4.2 EXPERIMENTAL

4.2.1 DYNAMIC MECHANICAL ANALYSIS

The thermomechanical behaviour of the SMP in bulk form was established using a dynamic mechanical analyser (DMA), Model Q800 from TA Instruments. Conditioned and unconditioned specimens of nominal dimensions 22 mm (length) x 15 mm (width) x 3.2 mm (thickness) were tested in torsion mode. DMA testing established the thermomechanical characteristics of the SMP for a range of temperatures (25°C to 130°C). The specimens were heated at a rate of 2°C/min, and an applied strain of 0.1% was oscillated at a frequency of 1 Hz.

4.2.2 NANOINDENTATION TESTS

The current study utilized a Nano Indenter XP (MTS NanoInstruments, Oak Ridge, TN) located at the Air Force Research Lab's Materials and Manufacturing Directorate, Wright-Patterson Air Force Base Dayton, OH. Figure 4.1 is a schematic representing the indenter apparatus and the indenter head mechanism. The indenter head assembly is

supported by two springs, which cause a very low vertical stiffness while maintaining a very large horizontal stiffness. The indenter shaft is a load-controlled solenoid armature, passing through an electromagnetic coil. Load force is then directly proportional to level of current passing through the coil. Displacement measurements are determined through a capacitive displacement gauge, which consists of three vertically concentric circular plates. The vertical displacement can be found by measuring the electric potential across the center plate and either of the other plates (MTS, 2004).

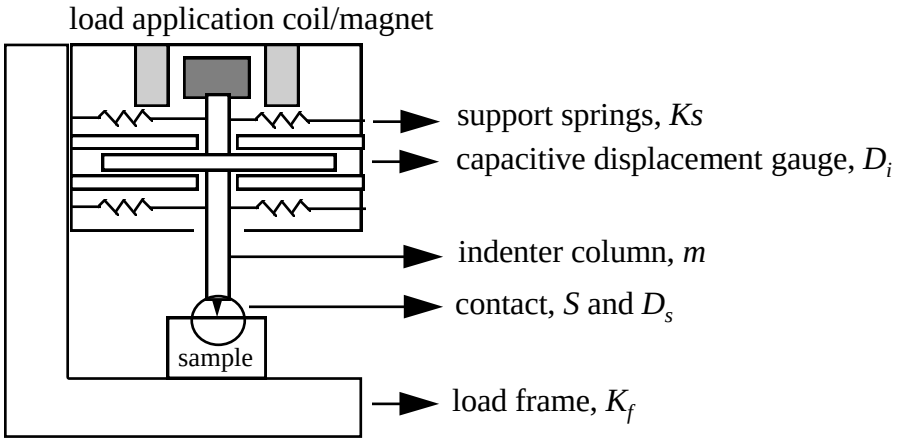

Figure 4.1. Schematic of the indenter mechanism for MTS Nano Indenter XP (MTS, 2004).

The Nano Indenter XP gantry (Figure 4.2) houses and supports the indenter head assembly, indenter shaft, and optics. The gantry is manufactured to be very rigid, which provides very high load frame stiffness. The load frame stiffness is crucial to the nanoindentation method. The gantry itself is installed inside an isolation cabinet and mounted on a MTS Minus K Table. Great care is taken to suppress any environmental disturbances that may affect the nanoindentation process. The isolation cabinet provides a controlled air mass that prevents sudden changes in temperature, and its foam lining absorbs acoustic energy to decrease acoustic transmission (Ripberger et al., 2004).

The gantry contains the main indenter assembly along with the optical viewing system, horizontal motion system, and sample holder. The optical system consists of a

microscope body with interchangeable 10X and 40X zoom lenses, a video camera, and a computer operated focus motor. A separate halogen light provides a light source that is controlled by an external remote. The motion system utilizing an X-Y directional stage to move and locate test samples under the microscope/video camera and under the indenter assembly.

Figure 4.2. Photograph of the MTS Nano Indenter XP gantry and isolation cabinet.

For these nanoindentation tests the SMP specimens were attached to testing disks with high-temperature adhesive (Poly-2000) having a low coefficient of thermal expansion. Each testing disk was then loaded into the aluminium testing stage (Figure 4.3). A Berkovich diamond indenter was used in the present experiments. The indenter has a nominal tip radius <20 nm and an inclined angle of 65.3 (degree).

Figure 4.3. Image of aluminium testing stage used for modulus measurements.

Polymeric materials exhibit viscoelastic characteristics (i.e. creep) when deformed. When performing nanoindentation on a viscoelastic material, the resulting load-depth curve exhibits a "bulge" in the initial unloading segment due to the excessive deformation caused by viscous creep. The occurrence of the "bulge" at the onset of unloading causes the contact stiffness (S) to be negative. Furthermore, the negative contact stiffness leads to inaccuracy when calculating the elastic modulus and hardness (Feng and Ngan, 2002). Conditions for the occurrence of the "bulge" have been found to be connected to overall load and loading/unloading rates (Ngan and Tang, 2002). Extensive work has been done to develop methods to minimize the effect of viscous creep and thermal drift (relevant at elevated temperatures). The "hold-at-the-peak" method (Figure 4.4) was developed to allow for more accurate measurements during depth-sensing tests of viscoelastic materials (Ngan et al., 2004; Tang and Ngan, 2003; Briscoe, et al., 1998; Fujisawa and Swain, 2006). The "hold-at-the-peak" method consists of holding the material at maximum load for a length of time before unloading.

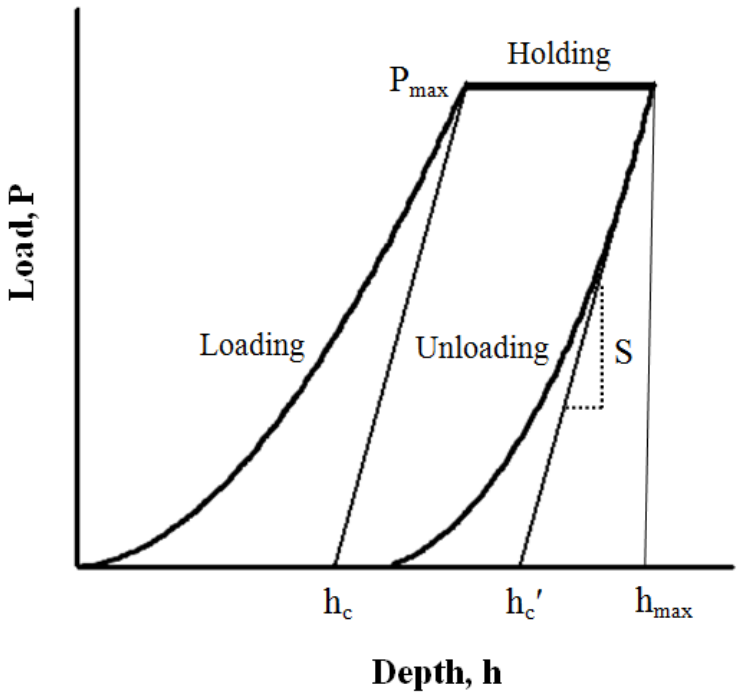

Figure 4.4. A diagram representing the "hold-at-the-peak" method used for nanoindentation of viscoelastic materials.

For the current experiments, the indenter was loaded at rates of 50 mN/s and 10 mN/s to a maximum load of 100 mN, and then held at the maximum load for a length of time (10 s). Using this method the initial "bulge" was no longer present in the final load-depth curves. The contact stiffness (S) was then computed using standard Oliver-Pharr method (1992, 2004).

The indentation depth caused by viscous creep, as well as the initial unloading rate and creep rate, need to be taken into account for the indenter-sample contact depth (h_c) calculation, as detailed in (Lu et al., 2009).

$$h_c = (h_{max} - h_{creep}) - 0.75P_{max}\left(\frac{1}{S} - \frac{\dot{h}}{\dot{P}}\right) \tag{4.1}$$

where $h_{\max}$ is the maximum indentation depth, h_{creep} the change in the indentation depth during the indenter holding time, $P_{\max}$ the peak load, S is the apparent stiffness that is determined from the slope of the unloading curve evaluated at the maximum depth ($S = (dP/dh)_{h=h_{max}}$), $\dot{h}$ is the creep rate at the end of the load hold, $\dot{h} = \partial h/\partial t$, and $\dot{P}$ the indenter unloading rate, $\dot{P} = \partial P/\partial t$.

After the correct contact depth is known, the indenter-sample contact area, A, can be estimated through a tip-area function (Oliver and Pharr, 1992). The tip-area function is an experimentally determined function of the contact depth

$$A = C_0 h_c^2 + C_1 h_c \tag{4.2}$$

where C_0 and C_1 are coefficients determined through a calibration process on a reference material. In the present experiments, the first two coefficients were determined by testing high-purity fused silica resulting in C_0=24.42 and C_1=712. Finally, the elastic modulus E of the testing sample was calculated using Equations (4.3a and 4.3b):

$$E_r = \frac{S\sqrt{\pi}}{2(1.034)\sqrt{A}} \tag{4.3a}$$

$$E = \frac{1-\nu^2}{\frac{1}{E_r} - \frac{1-\nu_i^2}{E_i}} \tag{4.3b}$$

where E_r is the reduced modulus, and E_i and ν_i are the elastic modulus and Poisson's ratio of the indenter (for diamond indenter: E_i=1140 GPa and ν_i=0.07). The Poisson's ratio, ν was assumed to be 0.35 for the current SMP.

4.3 RESULTS AND DISCUSSION

4.3.1 THERMOMECHANICAL PROPERTIES (DMA)

Dynamic mechanical analysis was used to determine the storage modulus and transition temperature of the SMP (Figure 4.5). The glass transition temperature of the SMP was determined by measuring the peak of the tan(δ) curve versus temperature. By definition, tan(δ) is the ratio of loss to the storage modulus, which were obtained using a DMA.

Figure 4.6 depicts the tan(δ) curves of the unconditioned and conditioned SMP specimens. Figure 4.7 shows the measured T_g values for the various conditions evaluated. It appears that all the conditioned SMPs exhibit a decrease in T_g as compared to the unconditioned one. Among them, the UV exposed and water immersed SMPs have the largest drops in T_g.

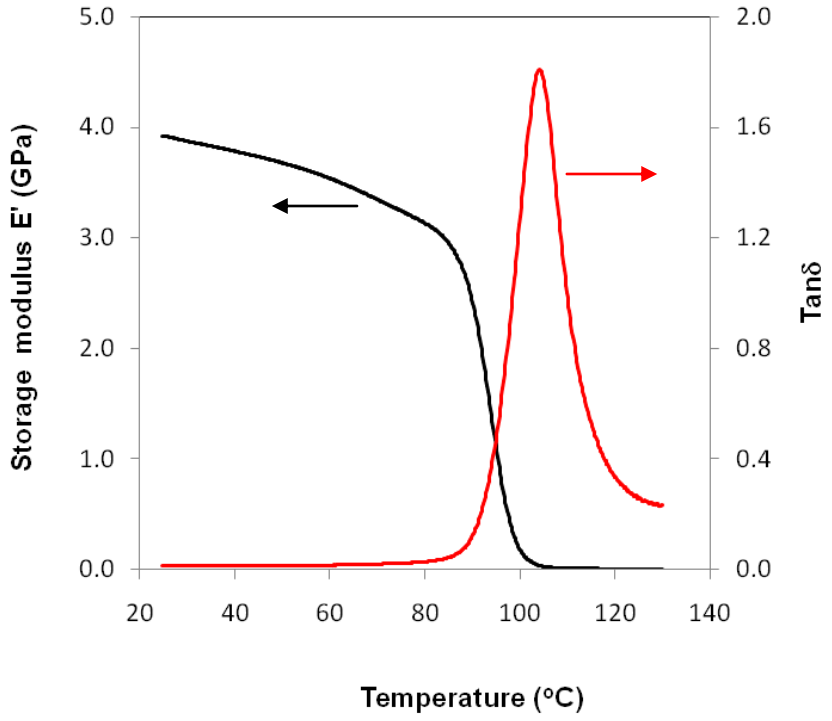

Figure 4.5. Resulting plot of the storage modulus and tanδ curves.

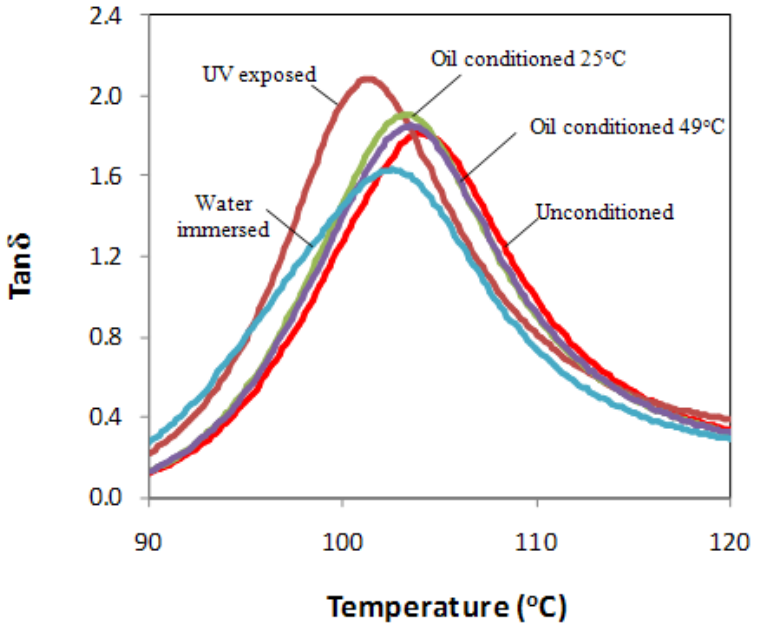

Figure 4.6. Tan(δ) curves of the unconditioned and conditioned SMP specimens measured using the DMA in torsion mode.

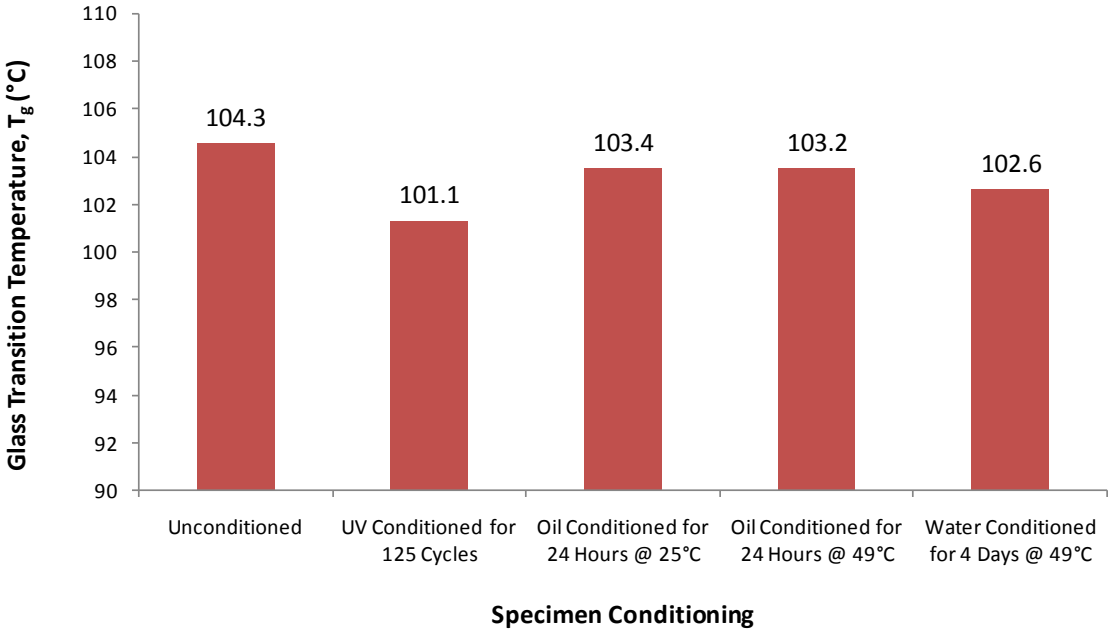

Figure 4.7. Glass transition temperatures of the unconditioned and conditioned SMPs obtained from peaks in tan(δ) curves.

4.3.2 Elastic Modulus (Nanoindentation Test)

The elastic modulus of the conditioned SMP was examined with a sharp (Berkovich) indenter. The typical indentation load-depth response for the unconditioned SMP is shown in Figure 4.8. The indenter loading rate was kept low at 10 mN/s, and the indenter holding time was 10 s. It is observed that viscous creep occurs during the indenter holding period, as shown in the inset in Figure 4.8, indicating that the indentation depth continues to increase during this time period.

The indentation depth caused by viscous creep, as well as the initial unloading rate and creep rate were all obtained from Figure 4.8, which allowed the calculation of the indenter-sample contact depth (h_c) by using Equation 4.1. Once h_c is obtained, the modulus of the SMP can be computed using Equation 4.3. The elastic modulus for the unconditioned SMP is calculated as 4.1 GPa, which is close to the storage modulus obtained from the DMA measurement (Figure 4.5).

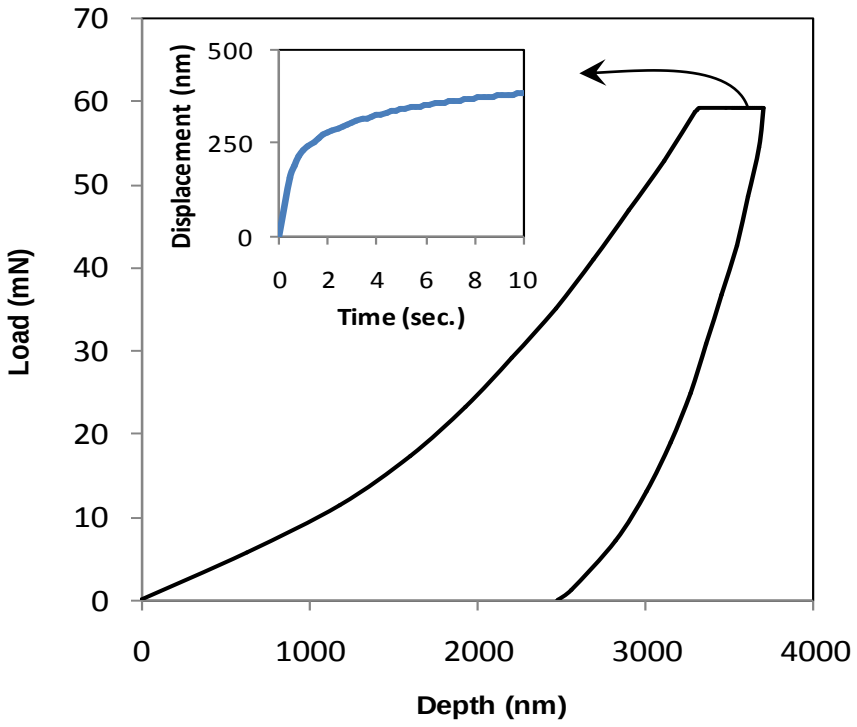

Figure 4.8. Indentation load-depth responses of the unconditioned SMP with a Berkvoich indenter at room temperature. The loading rate is 10 mN/s.

Nanoindentation tests were then performed at two different loading rates to help characterize the mechanical response of the conditioned SMPs. Resulting load-depth curves reveal that loading rates affect the resulting contact stiffness, and thus variances in the elastic modulus were seen. Figure 4.9 and Figure 4.10 present the load-depth plots for a loading rate of 50 mN/s and 10 mN/s, respectively. It can be seen that the UV exposed and water conditioned samples exhibit stiffer load-depth curves than the unconditioned sample.

The reported values for the elastic modulus are the average of at least 10 indents for each case considered. Figure 4.11 shows the measured elastic modulus values for the unconditioned and conditioned SMP. The nanoindentation tests were conducted at two different loading rates: 50 mN/s and 10 mN/s. Since viscoelastic materials are time-dependent, changing the loading rate results in variations in the responses of the SMPs. As expected, the material stiffness is seen to decrease with a slower loading rate for all conditions.

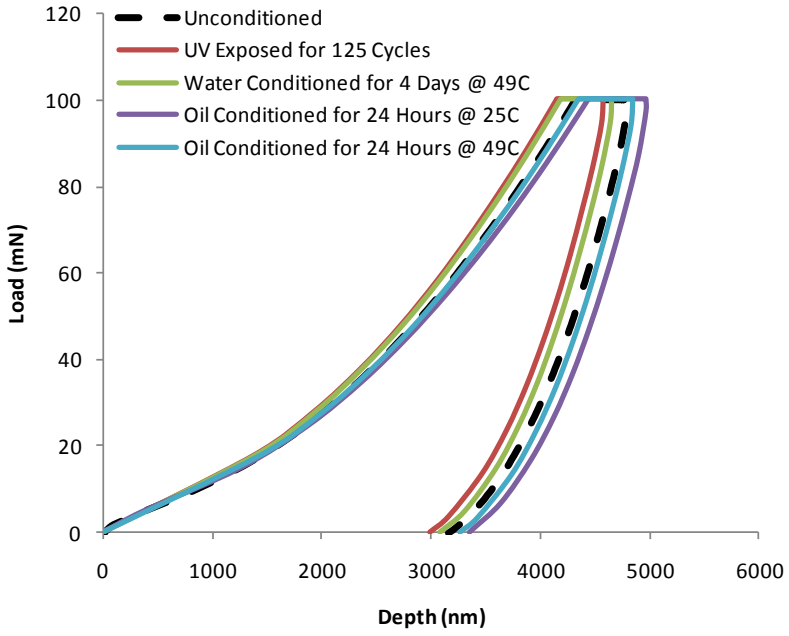

Figure 4.9. Load-depth curve corresponding to a loading rate of 50 mN/s.

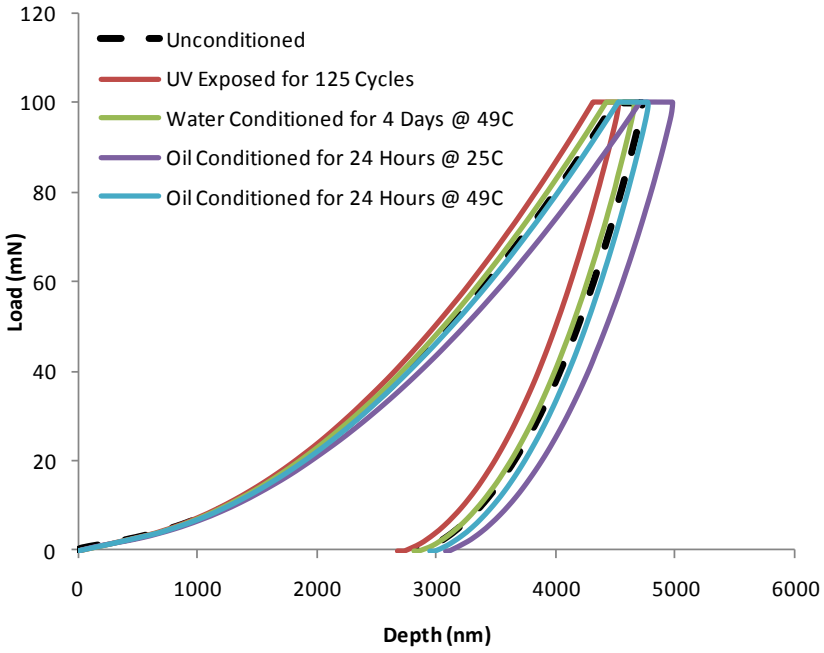

Figure 4.10. Load-depth curve corresponding to a loading rate of 10 mN/s.

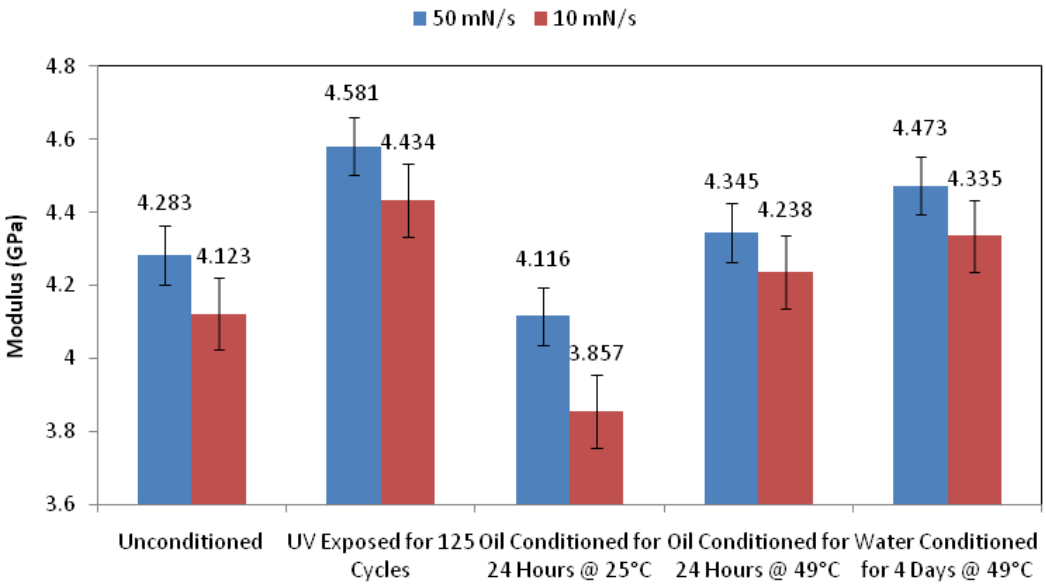

Figure 4.11. Elastic moduli of unconditioned and conditioned SMP using nanoindentation.

The elastic modulus of the unconditioned SMP was calculated to be 4.1~4.2 GPa, which is in good agreement with the storage modulus at room temperature (Figure 4.5). In most cases, the conditioned specimens have higher modulus than the unconditioned specimen, with the UV exposed and water conditioned specimens having the largest increase. This increase in material stiffness could be attributed to the onset of brittleness. The UV exposed sample did display a visible change in surface quality and color, so the UV radiation may cause a reaction with the polymer resin. Only SMP conditioned in oil at 25^{o}C seems to have a slightly lower modulus than the unconditioned specimen. These reported trends in elastic modulus values with conditioning are consistent with those obtained from macroscopic tensile tests by Tandon et al. (2009).

Statistical analysis was performed on the modulus measurements to determine whether or not the environmental conditioning has an effect on material performance. The analysis was conducted by using statistical software Design-Expert from Stat-Ease Inc. (2009) and the analysis of variance (ANOVA) result is shown in Table 4.1. Within 95% confidence level, a P-value less than 0.05 indicates that the modal factor is significant. The P-value from the present experiment is <0.0001, indicating that the environmental conditioning does have significant effect on the modulus of the SMP resin. Multiple pair-wise comparisons have been further performed by using Fisher's Least Significant Difference (LSD) Method (Table 4.2). Results have shown that the means (in modulus) from all treatments (environmental conditioning) are all different significantly.

Table 4.1. Analysis of Variance (ANOVA) for elastic modulus experiments on conditioned SMPs.

Source	**Sum of Squares**	**Degree of Freedom**	**Mean Square**	**p-value**
Environmental Conditioning significant	1.79	4	0.45	< 0.0001
Pure Error	0.041	40	1.013E-003	
Total	1.83	44		

Table 4.2. Multiple piece-wise comparisons for elastic moduli of environmentally conditioned SMPs.

Treatment Means	Estimated Mean	Standard Error
1 - Unconditioned	4.12	0.011
2 - UV Exposed	4.43	0.011
3 - Oil Conditioned 25^{o}C	4.24	0.011
4 - Oil Conditioned 49^{o}C	3.86	0.011
5 - Water Conditioned	4.34	0.011

Mean Treatment Difference	df	Standard Error	t for H_0 Coeff=0	Prob > |t|
1 vs 2	-0.31	0.015	-20.78	< 0.0001
1 vs 3	-0.12	0.015	-8.03	< 0.0001
1 vs 4	0.27	0.015	17.72	< 0.0001
1 vs 5	-0.21	0.015	-14.23	< 0.0001
2 vs 3	0.19	0.015	12.75	< 0.0001
2 vs 4	0.58	0.015	38.50	< 0.0001
2 vs 5	0.098	0.015	6.55	< 0.0001
3 vs 4	0.39	0.015	25.75	< 0.0001
3 vs 5	-0.093	0.015	-6.20	< 0.0001
4 vs 5	-0.48	0.015	-31.95	< 0.0001

4.4 CONCLUSIONS

Being able to characterize thermomechanical response and variation of mechanical properties of SMPs exposed to expected service conditions is essential to the advancement of reconfigurable air vehicles. Through dynamic mechanical analysis and

nanoindentation the thermomechanical response and mechanical properties of environmentally conditioned SMPs were examined. The resulting thermomechanical characterization revealed that upon conditioning the value of the transition temperature decreases for all conditions. It was also found that the elastic modulus varied according to the loading rate used for the nanoindentation experiment. However, the elastic moduli still follow the same trends independent of the loading rate. In most cases, the elastic modulus increases upon environmentally conditioning, with the UV exposed sample having the greatest increase. The results for the UV exposed specimen indicate the development of brittleness, which may be caused by a reaction between the UV radiation and the polymer resin. According to the present study, in-service conditions can significantly affect the thermomechanical and material response of SMPs.

CHAPTER FIVE SHAPE RECOVERY ABILITY OF ENVIRONMENTALLY CONDITIONED SMPS

5.1 INTRODUCTION

In this chapter the shape recovery ability of the conditioned and unconditioned SMP is explored through a novel high temperature nanoindentation technique. SMP recovery has been widely studied, but most correspond to deformation at temperatures below T_g (ambient temperatures) (Nelson and King, 2005; Wornyo et al., 2007; Yang et al., 2008). However, deforming SMPs at ambient conditions does not follow the proposed thermomechanical cycle (Figure 2.1) and could conceal important information on the recovery of SMPs. To follow the proposed thermomechanical cycle, a novel technique of high temperature nanoindentation was employed. Again, the MTS Nano Indenter XP, with modifications, was used to perform the indents at high temperature. The shape recovery response was considered using two styles of indenters: a Berkovich diamond tip indenter and a 300 μm diameter spherical indenter. To further characterize the shape recovery ability of the Veriflex-E SMP a range of recovery temperatures (T_r = 25°C, 60°C, 98°C, and 125°C) was used. During the recovery process a Wyko Optical Surface Profiler (Veeco Instruments Inc.) was utilized to perform a surface scan of the indent at each recovery temperature.

5.2 EXPERIMENTAL

5.2.1 HIGH TEMPERATURE NANOINDENTATION EQUIPMENT

Before performing the high temperature nanoindentation of the SMP the MTS Nano Indenter XP had to be modified with additional components. Instead of the standard testing stage, a MTS Localized High Temperature Stage (Figure 5.1) was utilized. The high temperature stage consists of aluminum base with a ceramic isolator, which houses the heating source. The ceramic isolator is attached to the aluminum base using a compression fit that is adjusted by tightening a bolt through the aluminum base. The heating source is comprised of two heater plates with a plated copper sample plate

attached to the top with four screws. The aluminum base also has ports for the circulation of a cooling fluid, which helps minimize the thermal effects of the surrounding system. Through circulation of the cooling media a more stable and precise thermal equilibrium can be achieved during testing. Cooling fluid is pumped through the heated stage by an external pump (Figure 5.2). The heating and cooling of the high temperature stage is controlled and monitored by a variable DC output proportional controller (Figure 5.3).

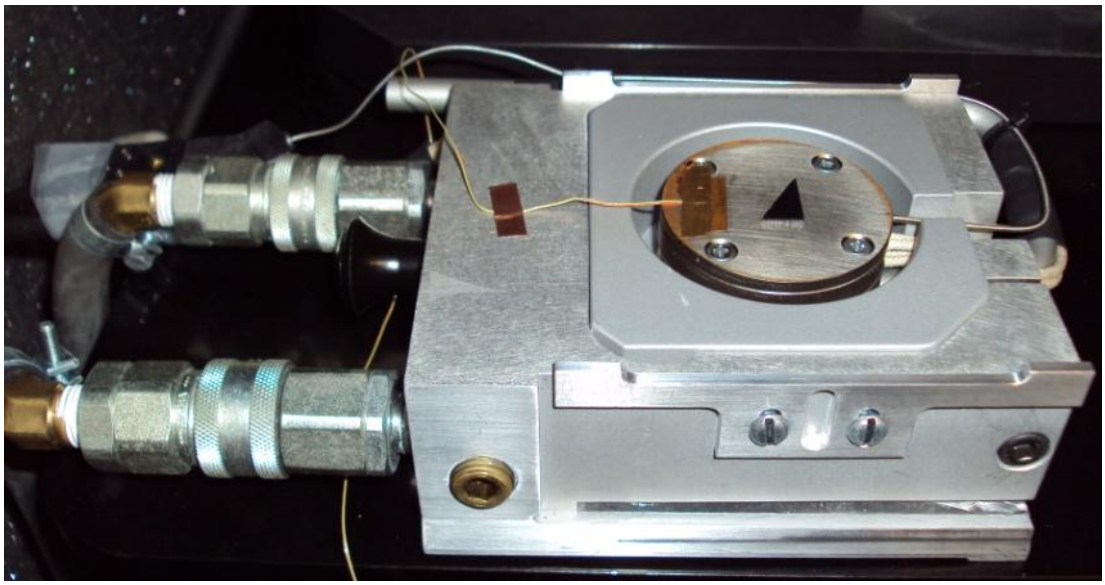

Figure 5.1. MTS Localized High Temperature Stage.

Figure 5.2. Coolant pump for the high temperature Nano Indenter XP.

Figure 5.3. Variable DC output proportional controller for high temperature Nano Indenter XP.

Due to the sensitivity and precision of the nano indenter assembly and the optical system a stainless steel heat shield (Figure 5.4) was installed to provide isolation from the heat source. A National Instruments CompactDAQ data acquisition system was used to improve temperature monitoring of the high temperature system. These additional thermocouple positions and application of LAB-VIEW software allowed for the sample temperature to be monitored in real-time throughout the testing procedure. This additional monitoring system is pictured in Figure 5.5.

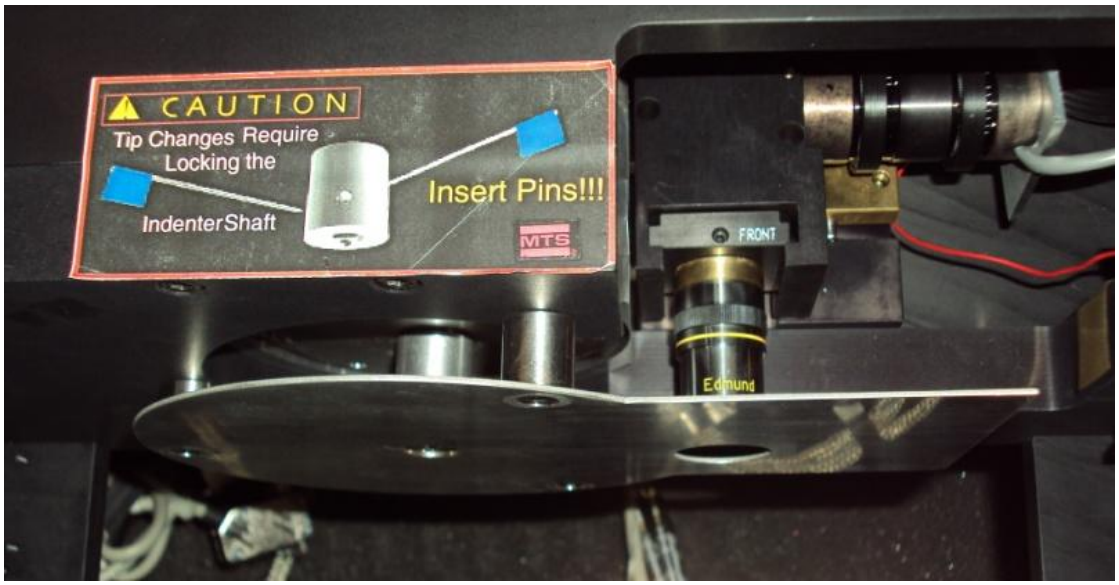

Figure 5.4. Heat shield installed on the MTS Nano Indenter XP.

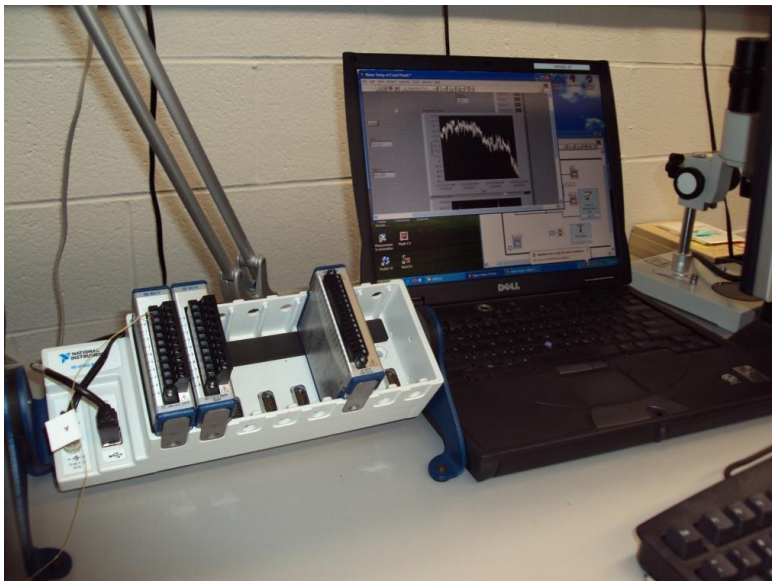

Figure 5.5. National Instruments CompactDAQ system and LAB-VIEW equipped laptop computer.

5.2.2 HIGH TEMPERATURE NANOINDENTATION TESTS

The shape recovery behavior of the SMP was examined according to the standard shape memory cycle (as shown in Figure 2.1) using a Berkovich diamond tip and a 300 μm diameter spherical tip. Figures 5.6 and 5.7 illustrate the proposed testing processes for the shape recovery analysis of the SMP utilizing the Berkovich diamond tip and the 300 μm diameter spherical tip, respectively. The first step of the process was to heat the SMP specimen to 110°C (T_d) using a heating rate of 2°C/min. The actual temperature of the specimen was monitored by a thermocouple placed near the specimen on the testing disk. The specimen was maintained at 110°C for at least 1 hr to assure thermal equilibrium within the sample. A loading rate of 5 mN/s was used to load the sample to a maximum load of 50 mN. Once the maximum load was achieved, the indenter was held at 50 mN while the sample was allowed to cool back to room temperature (T_s), and after reaching T_s the specimen was unloaded. It took approximately two hours for the sample to reach the room temperature after the heater was turned off.

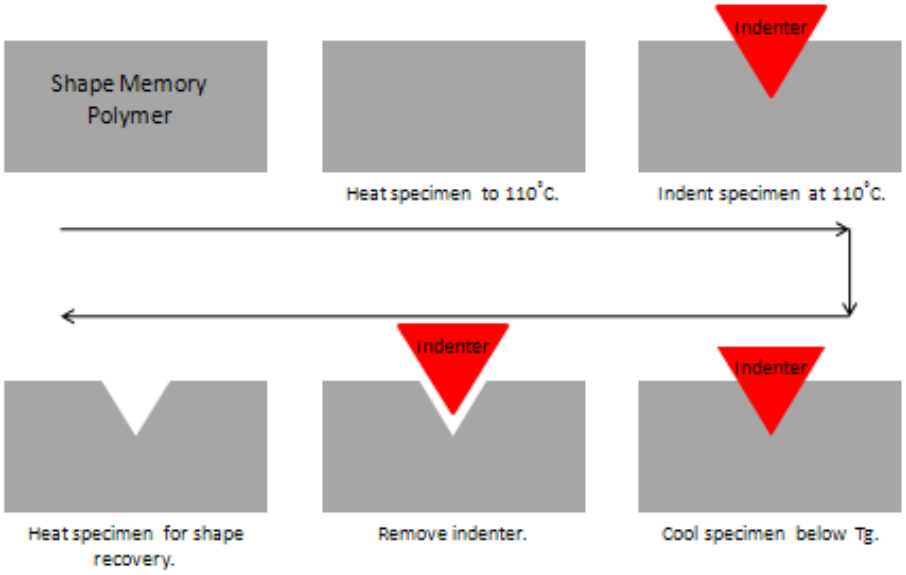

Figure 5.6. Illustration depicting the shape recovery experiment using high temperature nanoindentation with the Berkovich diamond tip.

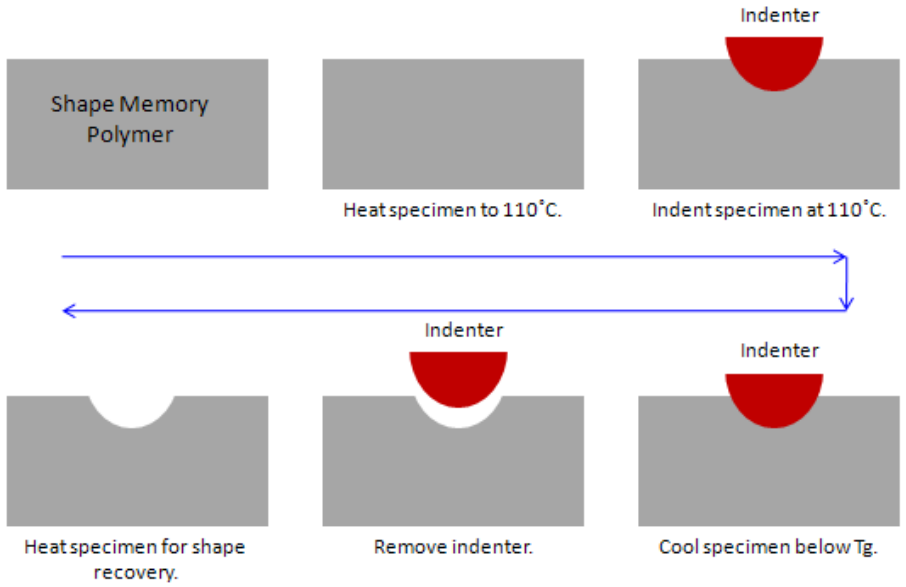

Figure 5.7. Illustration depicting the shape recovery experiment using high temperature nanoindentation with the spherical tip.

For a more qualitative and quantitative characterization of the shape recovery response of the SMP a Wyko Optical Surface Profiler (Veeco Instruments Inc.) was employed to scan the indentation profile of each sample during each stage of recovery. Figure 5.8 and Figure 5.9 represent the resulting indents created by the Berkovich tip and spherical tip, respectively , and the resulting depth profile scan.

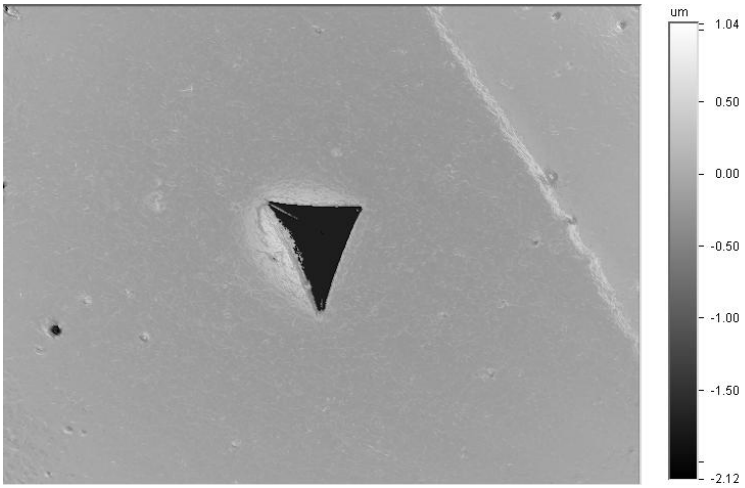

Figure 5.8. A scanned image of a Berkovich tip indent and the resulting depth profile.

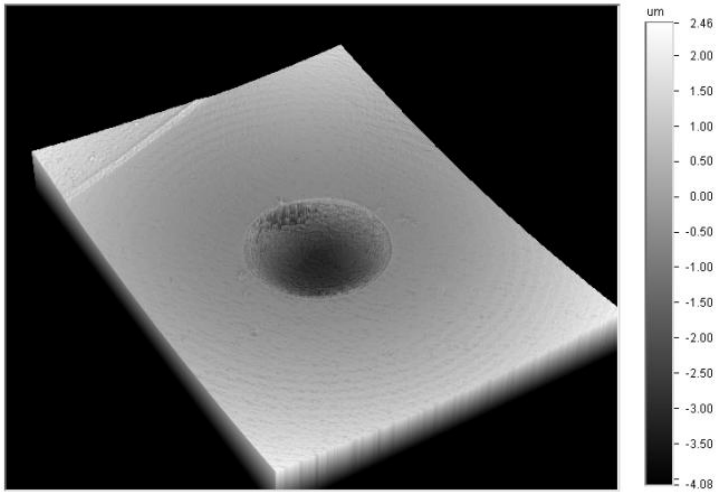

Figure 5.9. A scanned image of a spherical indent and the resulting depth profile scan.

Next the SMP sample was placed back on the high temperature stage to begin recovery. Recovery experiments were performed at several different temperatures (T_r: 60°C, 98°C, and 125°C) to help characterize the recovery ability of the SMP. As each SMP sample was heated, the optical system incorporated with the nanoindenter equipment was used to closely monitor the recovery process. Once the desired temperature was obtained, a 2-minute recovery time was used for all experiments. The SMP surface was then re-examined using the optical surface profiler to obtain the corresponding indentation profile and dimensions.

5.3 RESULTS AND DISCUSSION

The shape recovery ability of the SMP was examined by creating an indent and then observing the corresponding recovery according to the standard shape memory cycle. Recovery of the deformation was divided into several stages with an indentation profile being obtained at each stage. Each recovery stage was executed at a different recovery temperature (T_r: 60°C, 98°C, and 125°C). The indentation profile at each recovery temperature was analyzed by the Wyko Optical Surface Profiler.

5.3.1 SHAPE RECOVERY: BERKOVICH DIAMOND TIP

The first set of experiments performed involved the use of a Berkovich diamond tip indenter to create the high temperature indents. Figures 5.10-5.14 present a qualitative examination of the shape recovery ability of the SMP. The images shown are for the unconditioned sample and the conditioned samples. It can easily be seen that at temperatures well below T_g (T_r = 60°C) the recovery is very limited. Once the transition region is approached (T_r > 90°C), the recovery is seen to accelerate.

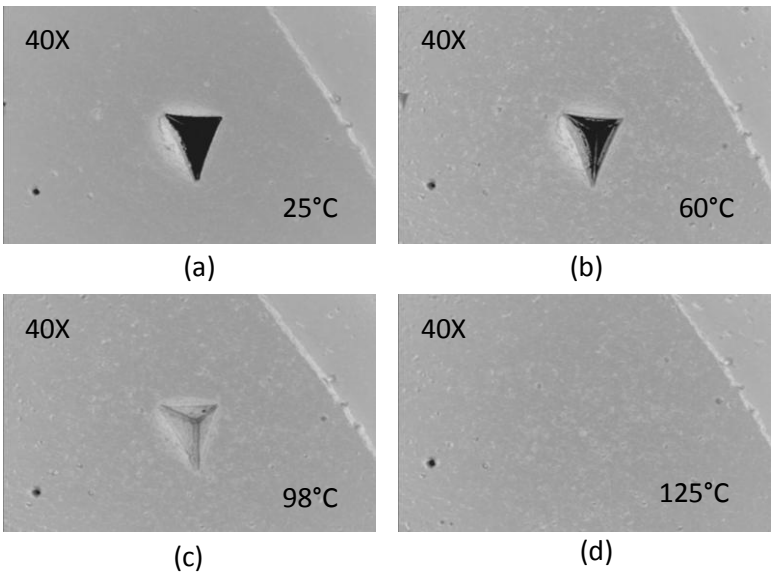

Figure 5.10. Composition of scanned indention images characterizing the shape recovery of the unconditioned SMP sample.

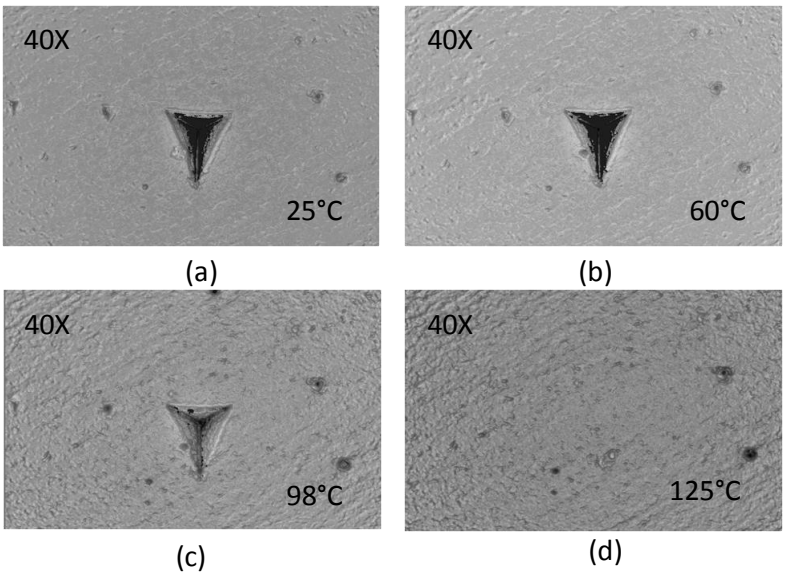

Figure 5.11. Composition of scanned indention images characterizing the shape recovery of the UV exposed SMP sample.

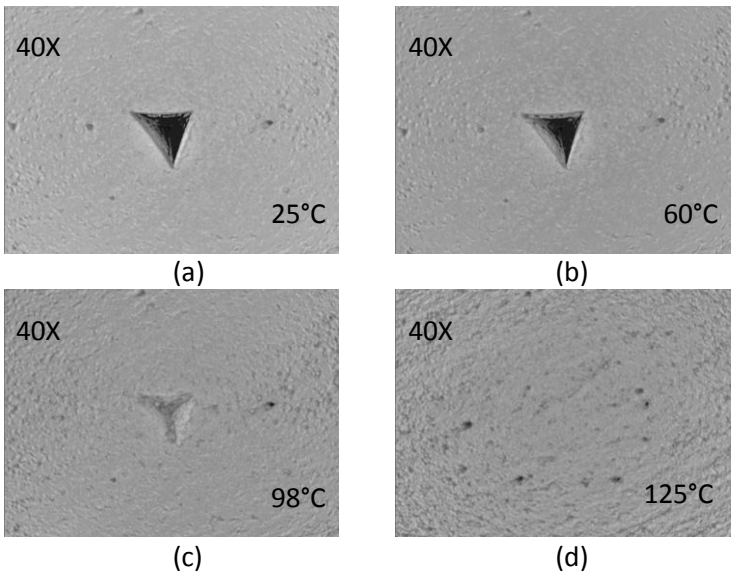

Figure 5.12. Composition of scanned indention images characterizing the shape recovery of the sample immersed in Oil at 25°C.

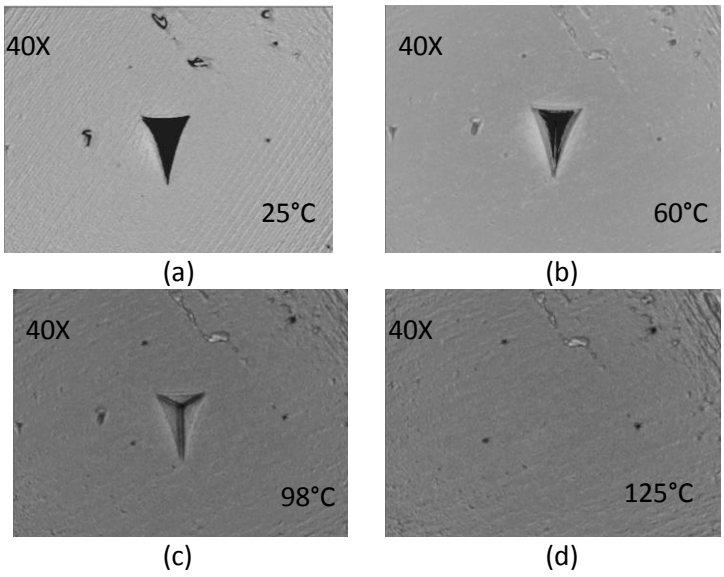

Figure 5.13. Composition of scanned indention images characterizing the shape recovery of the sample immersed in Oil at 49°C.

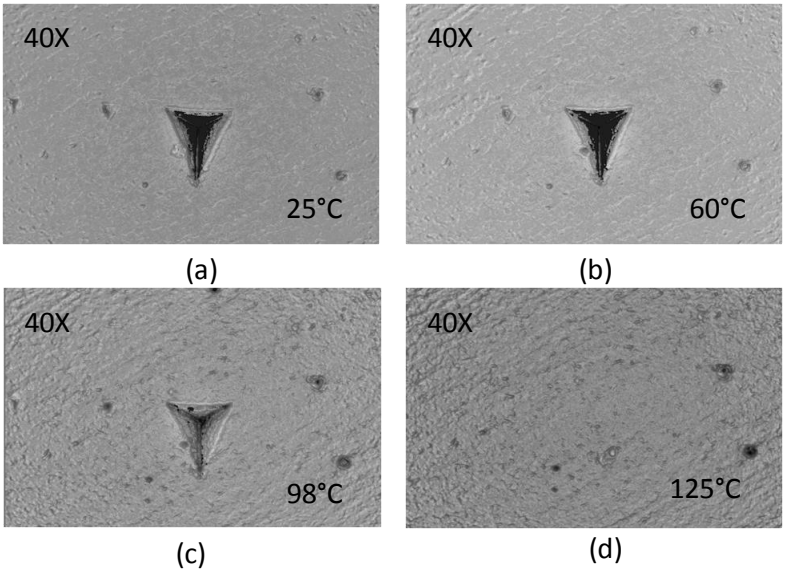

Figure 5.14. Composition of scanned indention images characterizing the shape recovery of the sample immersed in deionized Water at 49°C.

For a more quantitative approach the resulting scanned depth profiles were used to determine the indention size. Figure 5.15 is a diagram of a Berkovich tip indention and the corresponding measurements needed to determine the indentation size.

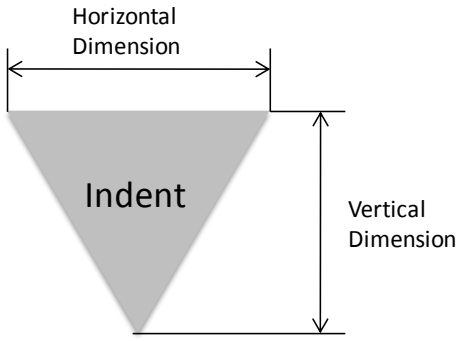

Figure 5.15. Schematic of measured dimensions for the Berkovich diamond tip shape recovery experiments.

Once the indentation size was measured, as illustrated in Figure 5.15, the indenter-sample contact area (A) was computed. Using Equation (5.1), the indentation contact depth (h_c) was found:

$$h_c = \frac{\sqrt{C_1^2 + 4C_0 A} - C_1}{2C_0} \tag{5.1}$$

where C_0=24.42, C_1=712 and A is the contact area estimated from the indentation profile. Though not completely accurate, this procedure provides a first order approximation of the indentation depth at each recovery temperature. The variation of indentation depth as a function of recovery temperature then provides an indication of the shape recovery ability of the SMP. Table 5.1 shows the resulting indentation depth at each recovery temperature for unconditioned and conditioned SMP specimens.

Table 5.1 Resulting indentation depths for SMP specimens during the Berkovich diamond tip shape recovery experiments.

Temp (°C)	**Indention Depth (μm)**				
	Unconditioned	UV Conditioned for 125 Cycles	Oil Conditioned for 24 Hours @ 25°C	Oil Conditioned for 24 Hours @ 49°C	Water Conditioned for 4 Days @ 49°C
25	3.55	3.65	3.86	3.68	3.79
60	3.52	3.65	3.82	3.64	3.70
98	3.29	3.57	3.27	3.36	3.47
125	≈ 0	≈ 0	≈ 0	≈ 0	≈ 0

Through evaluation of the indention depth the shape recovery is somewhat quantified, and again it is seen that the shape recovery is very limited, if not, non-existent below the transition region (T_r > 90°C). It can be seen that UV irradiated and water immersed specimens both have less recovery once the transition region is reached. However, once the recovery temperature approaches the transition temperature the specimens are seen to rapidly recover to nearly the original undeformed state for all conditions.

5.3.2 SHAPE RECOVERY: SPHERICAL TIP

To further improve the understanding of the shape recovery ability of the SMP a spherical tip indenter was utilized. Once more, the SMP samples were indented according the appropriate thermomechanical cycle shown in Figure 2.1. The spherical tip allowed for a more precise and accurate qualitative and quantitative assessment of the SMP's shape recovery ability, and also through indention with the spherical tip assessments on the durability of the SMP could be made. Figures 5.16-5.20 present resulting scanned depth profiles for the unconditioned and conditioned samples for the shaper recovery experiment using the spherical indenter. Just as with the Berkovich tip experiments the shape recovery is seen to be very limited at temperatures outside the transition region (T_r < 90°C).

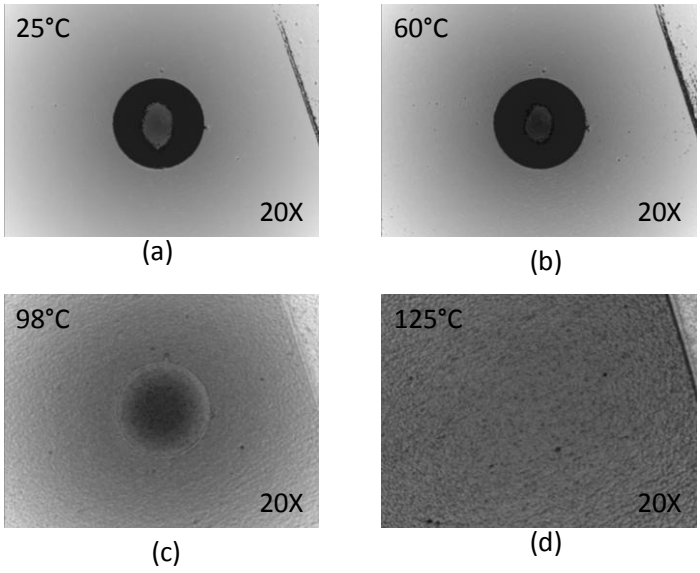

Figure 5.16. Composition of scanned depth images documenting the shape recovery process for the unconditioned SMP sample indented with the spherical tip: (a) 25°C, (b) 60°C, (c) 98°C, and (d) 125°C

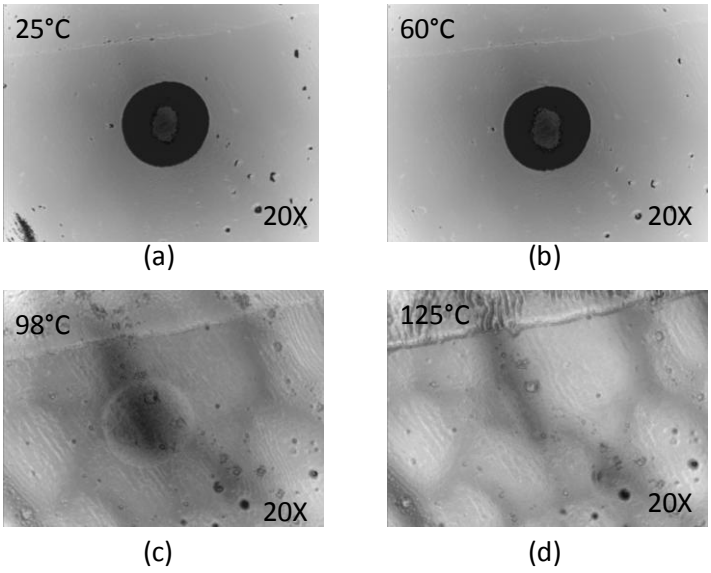

Figure 5.17. Composition of scanned depth images documenting the shape recovery process for UV-conditioned SMP sample indented with the spherical tip: (a) 25°C, (b) 60°C, (c) 98°C, and (d) 125°C.

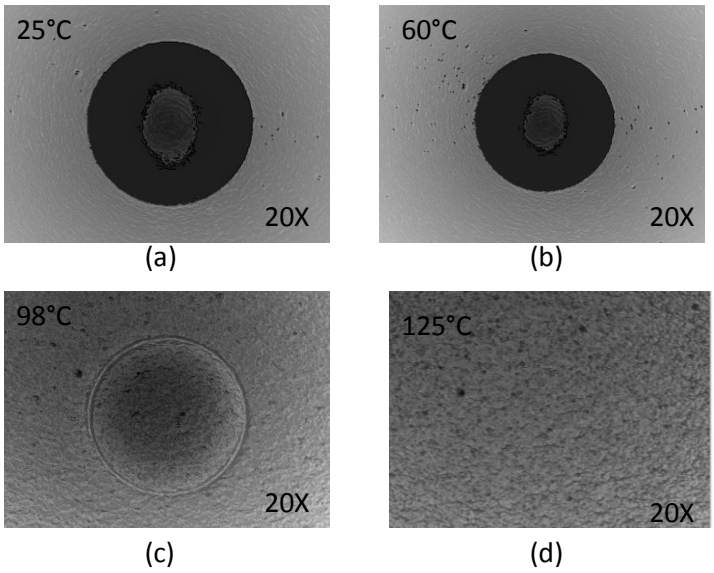

Figure 5.18. Composition of scanned depth images documenting the shape recovery process for oil, 25°C, conditioned SMP sample indented with the spherical tip: (a) 25°C, (b) 60°C, (c) 98°C, and (d) 125°C.

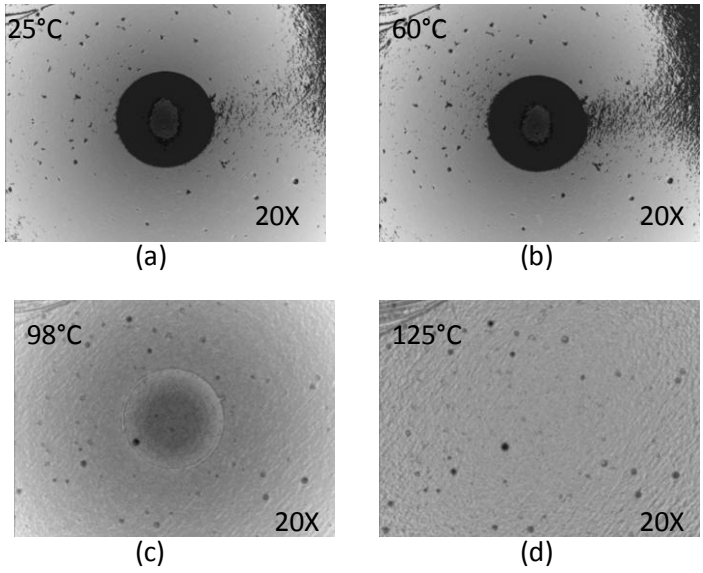

Figure 5.19. Composition of scanned depth images documenting the shape recovery process for oil, 49°C, conditioned SMP sample indented with the spherical tip: (a) 25°C, (b) 60°C, (c) 98°C, and (d) 125°C.

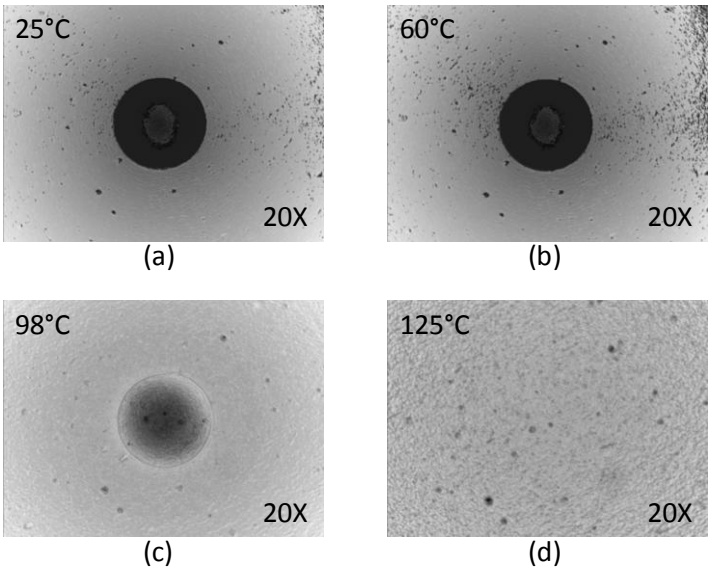

Figure 5.20. Composition of scanned depth images documenting the shape recovery process for water-conditioned SMP sample indented with the spherical tip: (a) 25°C, (b) 60°C, (c) 98°C, and (d) 125°C.

Another phenomenon seen when indenting the SMP with the spherical tip that was not apparent in the Berkovich tip experiments was appearance of "sink-in" deformation around the indent. Figure 5.15 shows an image of the SMP after being indented with the spherical tip and the corresponding indention, with the dashed vertical lines showing the indenter-specimen contact area. It is seen that the deformation zone has extended beyond the indenter-specimen contact. The indentation profile shows that the surface of the specimen has been substantially deformed. It indicates that there is a large amount of "sink-in" when indenting the SMP above its glass transition temperature. As $T_d > T_g$, the SMP is in a rubbery state and the deformation mechanism is mostly elastic. At low temperatures, the SMP is a rather rigid material and exhibits elastic-plastic type deformation. As a result, pile-up, rather than sink-in, has been often observed around the indentation. This kind of permanent deformation could be non-recoverable during subsequent heating, particularly at higher levels of stresses/strains. For the current experiment, the strain under a spherical indenter can be approximated by Equation 5.2.

$$\varepsilon_{ind} = 0.2 \cdot a / R \tag{5.2}$$

where a is the indenter-sample contact radius and R is the indenter radius. For the present SMP that was activated at 110°C, a is estimated at approximately 95.6 μm (based on the indentation profile, Figure 5.21), which corresponds to an indentation strain ε_{ind} = 20%. Considering that these indention experiments are compressive testing, 20% strain is a relatively high amount of strain. Once each sample was heated to above the transition temperature, near full recovery was achieved, and furthermore the shape recovery ability was unchanged by conditioning.

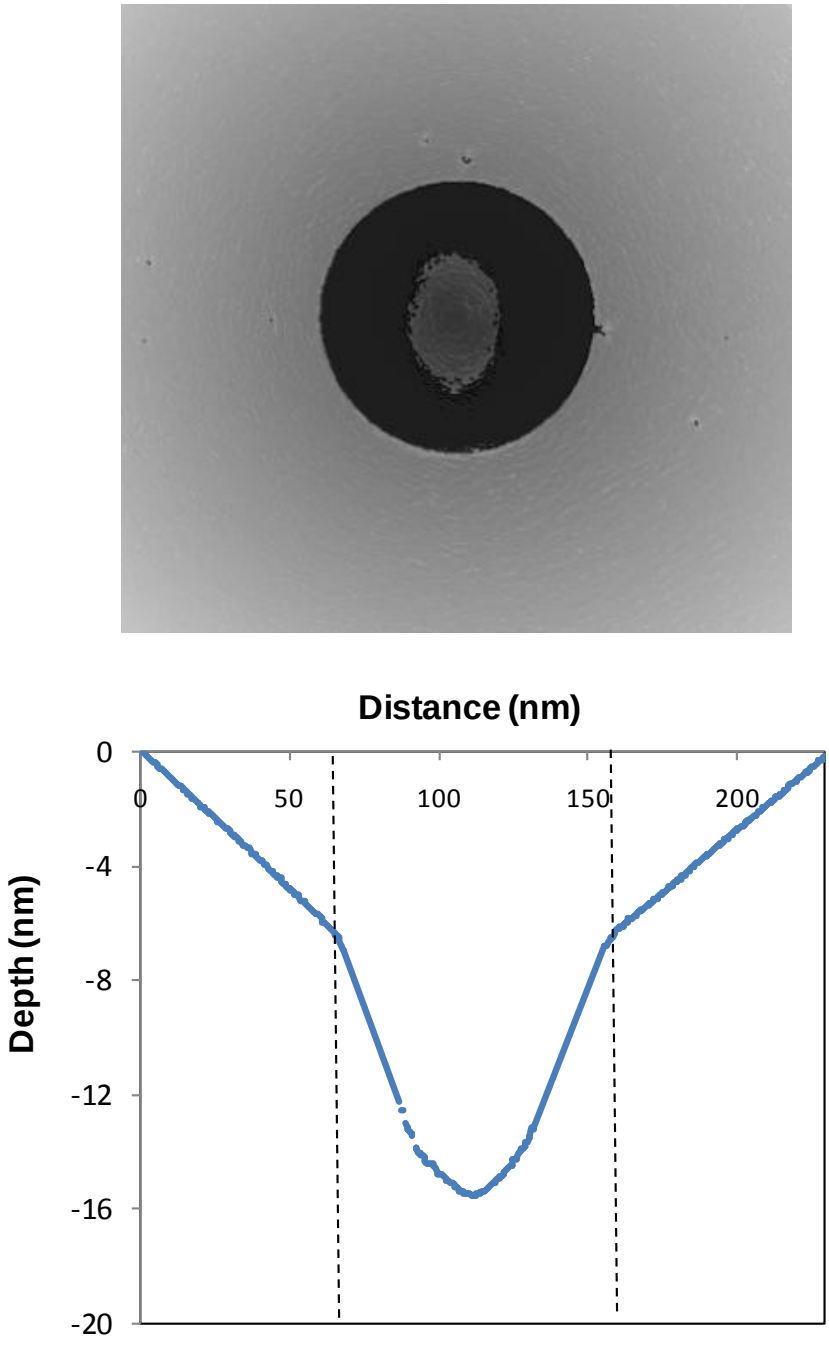

Figure 5.21. Indentation profile of the SMP after activated above the glass transition temperature (T_d=110°C).

5.3.3 SHAPE RECOVERY RATIO

The linear shape recovery ratio, R_{ur}, is a ratio of the recovered indention depth at a specified recovery temperature to the original indention depth. Evaluation of the linear shape recovery ratio provides a better quantitative assessment. The linear shape recovery ratio is determined by Equation 5.2.

$$R_{ur} = (1 - h_f / h_i) * 100 \tag{5.2}$$

where h_f is the final indentation depth corresponding to each recovery temperature and h_i is the initial indentation depth.

The indentation profiles of the SMPs at each recovery temperature have been measured with the Wyko Optical Surface Profiler, as shown in Figures 5.22-5.26, from which the initial indentation depth (h_i) and recovery indentation depth (h_f) are obtained. Using Equation 5.2, the linear shape recovery ratios are calculated for each SMP, as summarized in Table 5.2. It is seen that the indent recoveries are negligible when the material is in the glassy state (T_r: 25^{o}C, 60^{o}C). The resultant shape recovery ratios (R) are generally less than 1%. As the recovery temperature is increased above the onset of the glass transition, the indents begin to show significant recoveries. However, at T_r=98^{o}C, the UV exposed and water immersed SMPs have smaller recovery ratios in comparison to oil conditioned and the unconditioned resin (Table 5.2). Finally, as the SMP resin is re-heated above its T_g to 125^{o}C, the indents are nearly 100% recovered for all specimens. This indicates that the material's ability to regain shape remains relatively unchanged with conditioning, as long as the recovery temperature is above the T_g. Similar trends on shape recovery ratios have been reported by Tandon et al., who have conducted the shape recovery ability tests by using macroscopic tensile specimens.

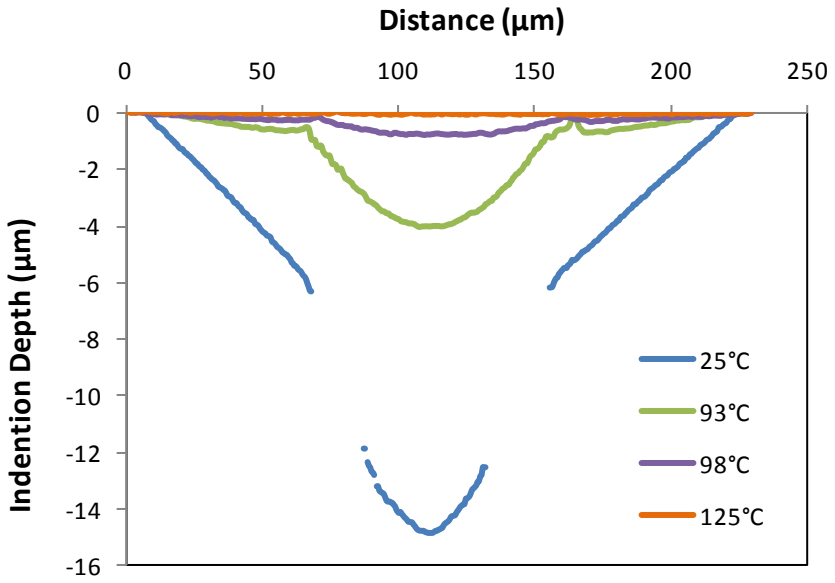

Figure 5.22. Indentation profiles for the unconditioned SMP sample indented with the spherical tip.

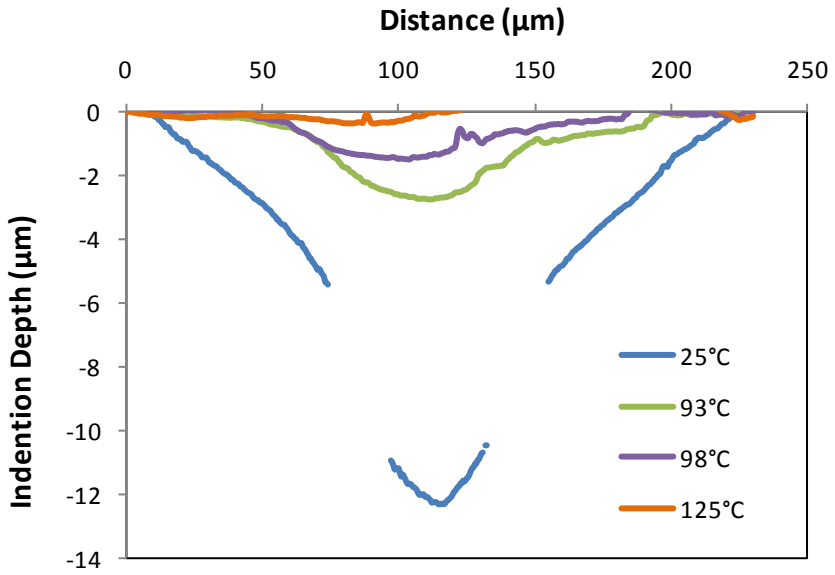

Figure 5.23. Indentation profiles for the UV exposed SMP sample indented with the spherical tip.

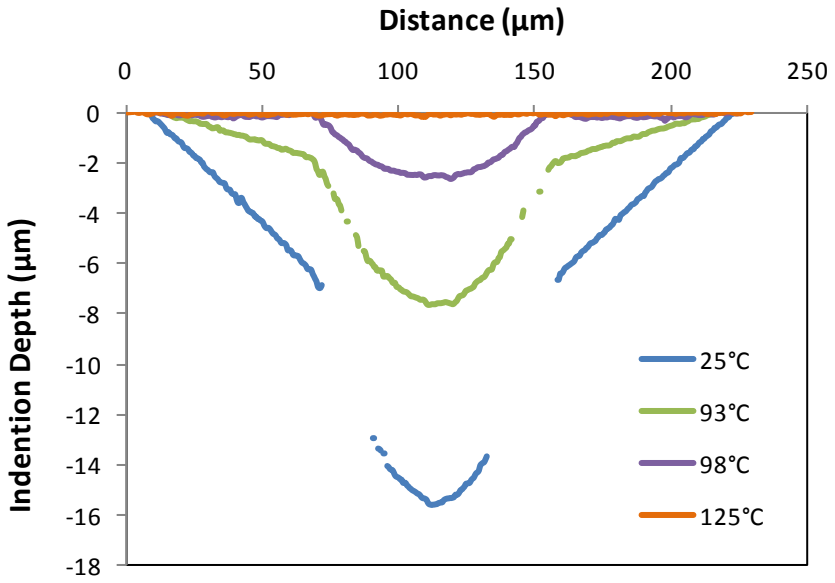

Figure 5.24. Indentation profiles for the water conditioned SMP sample indented with the spherical tip.

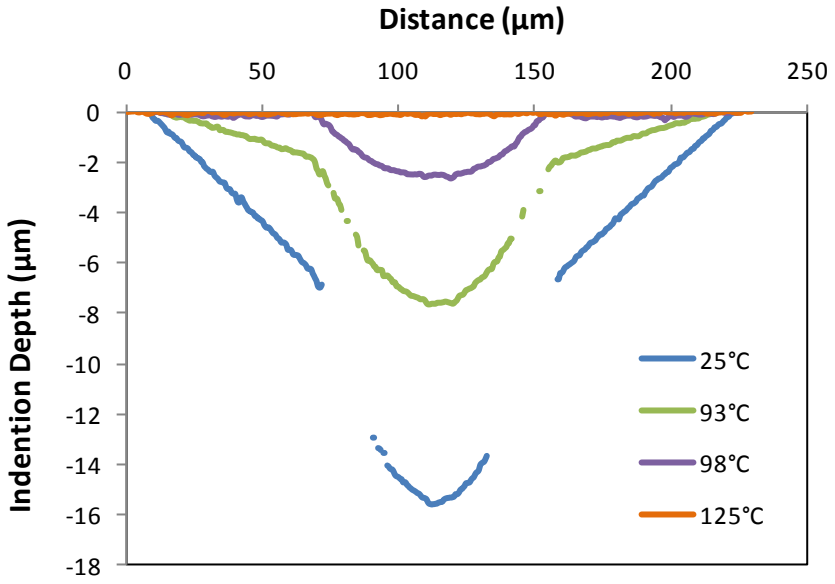

Figure 5.25. Indentation profiles for the oil, room temperature, conditioned SMP sample indented with the spherical tip.

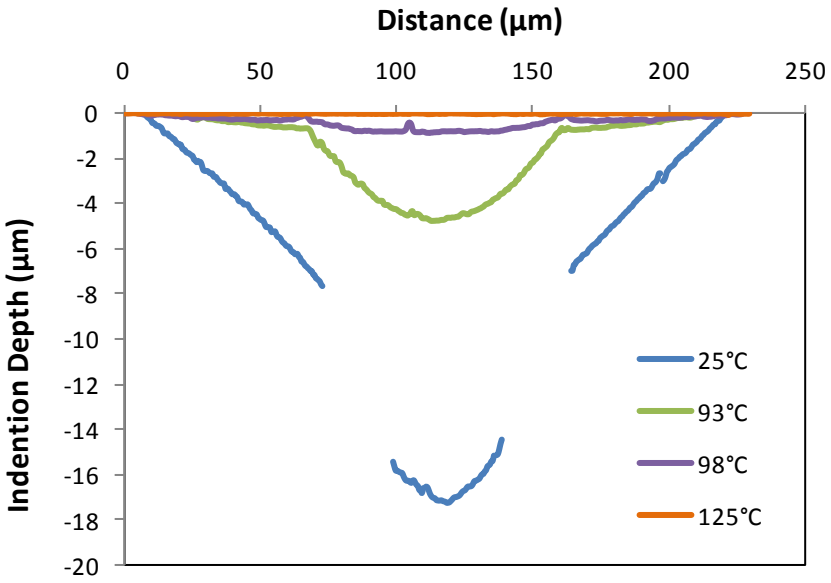

Figure 5.26. Indentation profiles for the oil, 49 ^{o}C, conditioned SMP sample indented with the spherical tip.

Table 5.2. Resulting linear shape recovery ratios for the unconditioned and conditioned SMPs indented with the spherical tip.

Temperature (°C)	Unconditioned	UV Conditioned for 125 Cycles	Oil Conditioned for 24 Hours @ 25°C	Oil Conditioned for 24 Hours @ 49°C	Water Conditioned for 4 Days @ 49°C
25	0	0	0	0	0
60	0.28	0.01	0.23	0.85	0.31
98	94.78	88.19	95.60	95.06	83.75
125	99.69	97.53	98.19	99.73	99.26

5.4 CONCLUSIONS

Through the use of novel high temperature nanoindentation techniques the shape recovery ability of the Veriflex-E SMP was characterized. Utilizing a Berkovich diamond tip and a 300 μm diameter spherical tip several shape recovery tests were executed. Testing with the Berkovich tip revealed that near full recovery was achieved at temperatures greater than the transition temperature ($T_r \geq 104°C$) independent of conditioning, however, at temperatures below the transition region ($T_r < 90°C$) the recovery is limited. The recovery trends seen in the shape recovery test using the spherical tip correspond directly with those seen in the Berkovich tip experiments. The accelerated shape recovery of the SMP once in the transition region is expected due to the fact that at temperature above T_g the SMP is in its "rubbery" state, which is dominated by elastic behaviour. However, below T_g the UV exposed and water immersed specimens had a slower recovery rate for both the sharp tip and spherical indenter experiments. At T_r= 98°C the two specimens were significantly less recovered than the other samples. Also, "sink-in" deformation rather than "pile-up" deformation was observed in the spherical tip experiments, which corresponds to the expected elastic behaviour of the SMP at elevated temperatures. Furthermore, the overall shape recovery ability of the Veriflex-E SMP is not dependent on environmental conditioning.

CHAPTER SIX SUMMARY OF CURRENT AND FUTURE WORK

6.1 WORK TO DATE

Shape memory polymers are a special class of active of materials that can recover their permanent shape from a temporarily deformed shape when exposed to an appropriate stimulus. The current study involved the thermomechanical characterization of a thermosetting two-part epoxy based SMP, Veriflex-E. Characterization was performed to examine the durability of the SMP for proposed application in highly adaptive air vehicles. According to Air Force testing procedures the SMP were conditioning according to expected service conditions, i.e. exposure to lubricants, water, and UV radiation. To further meet requirements for Air Force applications, each stage of conditioning was done at anticipated operation temperatures, 49°C or 120°F. Preliminary examination of the specimen after conditioning revealed that the UV exposed specimens developed a yellow tint and a drastic increase in surface roughness.

The thermomechanical properties of the SMP were examined using standard nanoindentation techniques and a Dynamic Mechanical Analyser (DMA). The transition temperature of the SMP was established through torsional DMA experiments. Results show that the transition temperature is lowered upon conditioning, with the water immersed and UV irradiated having the greatest decrease. Next the elastic modulus was measured using standard nanoindentation technique. Again, the modulus was seen to vary once the samples were conditioned. The water immersed and UV irradiated again have the greatest change, however, the modulus was seen to increase within these samples.

Novel high-temperature nanoindentation was used to characterize the shape recovery ability of the SMP. SMP shape recovery has been widely studied in recent years, but for most of those studies the samples were indented at ambient temperatures. According to the thermomechanical cycle of SMPs, deformation should take place after the specimen has been heated above the transition temperature. Failing to properly heat the specimen

before deformation could lead to unrecoverable deformation, so for this study the correct deformation procedure was performed for all shape recovery experiments. The shape recovery tests reveal that the recovery response of the SMP is relatively unchanged after conditioning.

6.2 FUTURE WORKS

With the current increase of interest in development of reconfigurable air vehicles, the advancement of research in the area of smart materials is paramount. The goal of the current study was to characterize the thermomechanical response of a SMP after being conditioned under anticipated service environments. Material properties including the transition temperature and elastic modulus, and shape recovery ability were examined to characterize any effect of service environment. The current experiments only involve investigation of material properties at the nano-scale. Further experimental work includes macro-scale investigations of the mechanical responses of the SMPs after being conditioned under anticipated service environments.

BIBLIOGRAPHY

1. Atli, B., Gandhi, F. and Karst, G. "Thermomechanical Characterization of Shape Memory Polymers," *Journal of Intelligent Material Systems and Structures*, 20(1):87-95 (2009).

2. Beake, B.D. and J.F. Smith, 2002. High-temperature nanoindentation testing of fused silica and other materials, *Philosophy Magazine*, A82, 2179.

3. Behl, M. and Lendlein, A. "Shape-Memory Polymers," *Materials Today*, 10(4):20-28 (2007).

4. Beloshenko, V. A., Varyukhin, V. N. and Voznyak, Y. V. "The Shape Memory Effect in Polymers," *Russian Chemical Review*, 74(3):265-283 (2005).

5. Briscoe, B.J., Fiori, L., Pelillo, E., "Nano-indentation of polymeric surfaces," *Journal of Physics D: Applied Physics*, 31, 1998, 2395-2405.

6. CRG Industries, LLC, Dayton, OH, 2010. http://www.crgrp.net/.

7. Feng, G., Ngan, A.H.W. "Effects of creep and thermal drift on modulus measurement using depth-sensing indentation," *Journal of Material Research*, 17(3):660-668 (2002).

8. Fujisawa, N., Swain, M.V., "Effect of unloading strain rate on the elastic modulus of a viscoelastic solid determined by nanoindentation," *Journal of Material Research*, 21(3):708-714, 2006.

9. Gall, K., Kreiner, P., Turner, D. and Hilse, M. 2004. Shape-Memory Polymers for Microelectromechanical Systems, *Journal of Microelectromechanical Systems*, 13(3), 472-483.

10. Huang, W. M., Ding, Z., Wang, C. C., Wei, J., Zhao, Y., Purnawali, H. "Shape memory materials," *Materials Today*, 13(7-8):54-51 (2010).

11. Kudva, J. N., "Overview of the DARPA Smart Wing Project," *Journal of Intelligent Material Systems and Structures*, 15:261-267 (2004).

12. McGowan, Anna-Maria R., Vicroy, Dan D., Busan, Ronald C., Hahn, Andrew S. "Perspectives on Highly Adaptive or Morphing Aircraft", NATO RTO AVT-168 Symposium, 20-24 Apr. 2009, Lisbon, Portugal.

13. Lendlein, A., and Kelch, S. "Shape-Memory Polymers," *Angew Chem. Int. Ed*., 41: 2034-2057 (2002).

14. Liu, C., Qin, H. and Mather, P. T. "Review of Progress in Shape-Memory Polymers," *Journal of Materials Chemistry*, 17:1543-1558 (2007).

15. Lu, Y.C., Jones, D. C., Tandon, G. P., Putthanarat, S. and Schoeppner, G. A. 2009. High Temperature Nanoindentation of PMR-15 Polyimide, *Experimental Mechanics*, (2009). DOI 10.1007/s11340-009-9254-5.

16. Meents, E.P.; Barnell, T.J.; Cable, K.M.; Margraf, T.W.; Havens, E. Self-healing reflexive composite structures for marine environments. In Proceedings of SAMPE 2009, Baltimore, MD, USA, 18–21 May 2009.

17. Nelson, B.A. and King, W.P. 2005. Shape Recovery of Nanoindentation Imprints in a Thermoset "Shape Memory" Polymer, *Applied Physics Letters*, 86, 103108.

18. Ngan, A.H.W, Tang, B., "Viscoelastic effects during unloading in depth-sensing indentation," *Journal of Material Research*, 17(10):2604-2610, 2002.

19. Ngan, A.H.W., Wang, H.T., Tang, B., Sze, K.Y., "Correcting power-law viscoelastic effects in elastic modulus measurement using depth-sensing indentation," *International Journal of Solids and Structures*, 42, (2005), 1831–1846.

20. Oliver, W.C. and Pharr, G.M., 1992, An improved technique for determining hardness and elastic modulus using load and displacement sensing indentation experiments, Journal of Materials Research, 7, 1564.

21. Oliver, W.C. and Pharr, G.M., 2004, Measurement of hardness and elastic modulus by instrumented indentation: advances in understanding and refinements to methodology, J Mater Res 19, pp. 3–20

22. Pretsch, T.; Jakob, I.; Müller, W. Hydrolytic degradation and functional stability of a segmented shape memory poly(ester urethane). Polym. Degradation Stability 2009, 94, 61-73.

23. Ratna, D. and Karger-Kocsis, J. “Recent Advances in Shape Memory Polymers and Composites: A Review,” *Journal of Materials Science*, 43:254-269 (2008).

24. Ripberger, E., Tandon, G. P., and Schoeppner, G. A., "Characterizing oxidative degradation of PMR-15 resin," in *S.A.M.P.E. 2004 Symposium and Exhibition*, Long Beach, CA, 2004.

25. Sawant, A. and Tin, S., 2008. High Temperature Nanoindnetation of a Re-Bearing Single Crystal Ni-Base Superalloy, *Scripta Materialia*, 58, 275-278.

26. Schuh, C. A., C. E. Packard, A. C. Lund, 2006. Nanoindentation and Contact-Mode Imaging at High Temperatures, *Journal of Materials Research*, 21, 725-736.

27. Tandon, G.P.; Goecke, K.; Cable, K.; Baur, J. Durability assessment of styrene- and epoxy-based shape-memory polymer resins. J. Intell. Mater. Sys. Struct. 2009, 20, 2127-2143.

28. Tang, B., Ngan, A.H.W, “Accurate measurement of tip-sample contact size during nanoindentation of viscoelastic materials,” *Journal of Material Research*, 18(5):1141-1148, 2003

29. Thill, C.; Etches, J.; Bond, I.; Potter, K.; Weaver, P. “Morphing skins,” *The Aeronautical Journal*, 2008, 112, 117-139.

30. Tobushi, H., Hara, H., Yamada, E., and Hayashi, S. “Thermomechanical Properties in a Thin Film of Shape Memory Polymer of Polyurethane Series,” *Smart Materials and Structures*, 5:483-491 (1996).

31. Tobushi, H., Hashimoto, T., Ito, N., Hayashi, S., and Yamada, E. “Shape Fixity and Shape Recovery in a Film of Shape Memory Polymer of Polyurethane Series,” *Journal of Intelligent Material Systems and Structures*, 9:127-136 (1998).

32. Volinsky, A.A., Moody, N.R. and Gerberich, W.W., 2004, Nanoindentation of Au and Pt/Cu Thin Films at Elevated Temperatures, *Journal of Materials Research*, 19(9), 2650-2657.

33. Wei, Z. G., Sandstrom, R. and Miyazaki, S. “Review Shape-Memory Materials and Hybrid Composites for Smart Systems, Part I Shape-Memory Materials,” *Journal of Materials Science*, 33:3743-3762 (1998).

34. Wornyo, E., Gall, K., Yang, F. and King, W.P. 2007. Nanoindentation of shape memory polymer networks, *Polymer*, Volume 48, Issue 11, 21, Pages 3213-3225.

35. Yang, F., Wornyo, E., Gall, K. and King, W.P. 2008. Thermomechanical Formulation and Recovery of Nanoindentation in a Shape Memory Polymer Studied Using a Heated Tip, *Scanning*, 30, 197-202.

VITA

JARED TERRELL FULCHER

Born June 10th 1986 in Nashville, Tennessee.

EDUCATION

MS, Mechanical Engineering, University of Kentucky (UK), Lexington, KY (May 2011)

BS, Suma cum Laude, Mechanical Engineering, University of Kentucky, Paducah, KY (May 2009)

AS, High Distinction, West Kentucky Community and Technical College, Paducah, KY (May 2007)

PROFESSIONAL EXPERIENCE

Graduate Research Assistant – 06/2009-Present
- Air Force Research Laboratory (AFRL) – Materials and Manufacturing Decorate, WPAFB, Dayton, OH
- University of Kentucky – College of Engineering, Lexington, KY

Lab Technician – 02/2006-06/2009
- UK College of Engineering Extended Campus Program, Paducah, KY

Design Engineer Intern – 05/2008-08/2008
- United State Enrichment Corporation, Inc., Paducah, KY

Plant Engineer Intern – 05/2007-07/2007
- Arkema, Inc., Calvert City, KY

AWARDS AND AFFILIATIONS

- Kentucky Space Grant Consortium
  - Graduate Fellowship – Fall 2009/Fall 2010

- American Society of Mechanical Engineers – University of Kentucky-Paducah, Paducah, KY
  - President – 2007/2009
  - Treasurer – 2006/2007
  - Design Competition Participant – 2007/2009

- Society of Automotive Engineers – University of Kentucky-Paducah, Paducah, KY
  - Reporter – 2008/2009

    - Baja SAE Crew Member – 2007/2009

- Pi Tau Sigma, National Mechanical Engineering Honor Society, Inducted Fall 2007

- Tau Beta Pi, National Engineering Honor Society, Inducted Fall 2007

- 3rd Place Undergraduate Research Division – American Society for Engineering Education, ASEE SE Annual Meeting, Southern Polytechnic State University, Marietta, GA (2009)

- Donn E. Hancher Senior Leadership Award – UK College of Engineering, Lexington, KY (Inaugural Recipient 2009)

- Outstanding Mechanical Engineering Student – UK College of Engineering Extended Campus, Paducah, KY (2009)

- Paducah Rotary Senior Scholar – UK College of Engineering Extended Campus, Paducah, KY (2009)

- J.M. Harper Memorial Engineering Scholarship – UK College of Engineering Extended Campus, Paducah, KY (Fall 2008/Spring 2009)

- White, E. Field Memorial Scholarship – UK College of Engineering, Lexington, KY (2008/2009)

- Dean's List – University of Kentucky, Lexington, KY (Fall 2007/Spring 2009)

- Hites Family Scholarship – West Kentucky Community and Technical College, Paducah, KY (Fall 2007/Spring 2009)

- Marvin Family Scholarship – UK College of Engineering Extended Campus, Paducah, KY (Fall 2007/Spring 2009)
- Trustees Scholarship – University of Kentucky, Lexington, KY (Fall 2007/Spring 2009)

- Paducah Kiwanis Sophomore Scholar- UK College of Engineering Extended Campus, Paducah, KY (2007)

- Dean's List – West Kentucky Community and Technical College, Paducah, KY (Fall 2005/Spring 2007)

PUBLICATIONS/PRESENTATIONS

Fulcher, J.T., Lu, Y.C., Tandon, G.P., Foster, D.C., "Thermomechanical characterization of shape memory polymers using high temperature nanoindentation", *Polymer Testing*, Volume 29, Issue 5, 08/10.

Fulcher, J.T., Lu, Y.C., Tandon, G.P., Foster, D.C., "Mechanical Characterization of Environmentally Conditioned Shape Memory Polymers by High Temperature Indentation", Presented at 2010 SEM Annual Conference & Exposition on Experimental and Applied Mechanics, Indianapolis, IN, 06/10.

Fulcher, J.T., Lu, Y.C., Tandon, G.P., Foster, D.C., "Shape Memory Effects of Environmentally Conditioned Shape Memory Polymers Studied by Nanoindentation", Presented at SAMPE 2010, Seattle, WA, 05/10.

Fulcher, J.T., Lu, Y.C., Tandon, G.P., Foster, D.C., "Thermomechanical Characterization of Environmentally Conditioned Shape Memory Polymer Using Nanoindentation", Presented at Proceedings of the SPIE Smart Structures / NDE Conference, San Diego, CA, 03/10.

Beadles, W. J., Fulcher, J. T., "Modal Analysis of an Engine Valve Cover: Experimental Testing and Finite Element Modeling", Technical Poster presented at ASEE SE Annual Meeting, Marietta, GA, 04/09.